Aus der Abteilung Neurologie Max-Planck-Institut für Kognitions- und Neurowissenschaften Leipzig

DISSERTATION

The Impact of Heart-Brain Interactions
on Somatosensory Perception

Der Einfluss von Herz-Hirn Interaktionen
auf die somatosensorische Wahrnehmung

zur Erlangung des akademischen Grades
Doctor of Philosophy (PhD)

vorgelegt der Medizinischen Fakultät Charité – Universitätsmedizin
Berlin

von

Esra Al
aus Kayseri, Turkei

Datum der Promotion: 26.06.2022

Table of contents

List of Abbreviations

EEG	Electroencephalography
MEG	Magnetoencephalography
ECG	Electrocardiography
HEP	Heartbeat-Evoked Potential
SEP	Somatosensory-Evoked Potential
HRV	Heart Rate Variability
SDT	Signal Detection Theory
FA	False Alarm
TMS	Transcranial Magnetic Stimulation
S1	Primary Somatosensory Cortex
PCC	Posterior Cingulate Cortex
ACC	Anterior Cingulate Cortex
rIPL	Right Inferior Parietal Lobule
LPFC	Lateral Prefrontal Cortices
NTS	Nucleus of the Solitary Tract
2AFC	Two-Alternative Forced-Choice
ICA	Independent Component Analysis
IC	Independent Component

1 Synopsis

1.1 Abstract (English)

Our perception of the external environment is affected by sensory stimuli and by the state of the brain. Interestingly, exteroception can also be influenced by *interoceptive* signals from the body. Specifically, heartbeat-related factors have been demonstrated to affect exteroception. However, so far it is poorly understood, which behavioral aspects and perceptual neural processes are affected by the heart. In this dissertation, we identify and characterize two heartbeat-related effects on somatosensory perception and their neural correlates. They are based on (i) stimulus timing along the cardiac cycle and (ii) the neural response to heartbeats, i.e., heartbeat-evoked potentials (HEP).

In the early phase of my PhD, I was a coauthor in a behavioral study (Motyka et al., 2019) showing that somatosensory stimuli were less often detected during systole relative to diastole phase of the cardiac cycle. This early work motivated us to further investigate the psychophysical and neural mechanisms underlying the effect of cardiac signals on somatosensory perception. To this end, in the main study of this thesis (Al et al., 2020) we tested, in 37 healthy subjects, both the influence of cardiac phase and prestimulus HEP amplitudes on somatosensory detection and localization in an electroencephalography (EEG) experiment.

The results of the main study first confirmed behaviorally the difference in somatosensory perception between systole and diastole. Using signal detection theory, we demonstrated that the lower perception in systole was related to a shift in perceptual sensitivity rather than in criterion (bias). Similar to detection, correct localization of somatosensory stimuli was also weaker during systole. In the EEG signals, weaker perception during systole coincided with smaller amplitudes of late components (P300) of the somatosensory-evoked potential (SEP). Secondly, we demonstrated that prestimulus HEP amplitudes were inversely related to stimulus localization and detection due to the adoption of a more conservative decision criterion. This effect was associated with changes in amplitudes of both early (P50) and late (N140, P300) SEP components. These two heartbeat-related effects were independent of the effect of alpha oscillations on somatosensory perception. We interpret cardiac phase effects in an interoceptive predictive coding framework and propose that HEP effects can be linked to spontaneous changes

between interoception and exteroception. In a follow-up EEG study (Al et al., 2020, *in revision*), we replicated these two distinct influences of heartbeat-related events on somatosensory detection and evoked potentials.

These two mechanisms of heart-brain interactions are important for understanding of how access to conscious perception is regulated. In the clinical domain, they may contribute to our understanding of cardiac complications after stroke and cognitive disturbances in cardiac disorders, issues to be investigated in future studies.

1.2   Abstract (Deutsch)

Unsere Wahrnehmung der Umwelt wird sowohl durch externe Reize als auch den momentanen Zustand des Gehirns bestimmt. Interessanterweise spielen auch interozeptive Signale des Körpers, insbesondere Herzschlag-bezogene Faktoren, eine wichtige Rolle. Es ist jedoch unklar, welche Aspekte des Verhaltens und neuronalen Korrelate der Wahrnehmung vom Herz beeinflusst werden. In der vorliegenden Dissertation werden zwei Herzschlag-bezogene Effekte auf die somatosensorische Wahrnehmung und ihre neuronalen Korrelate identifiziert und charakterisiert: (i) der Einfluss des Zeitpunkts der Stimulation während des Herzzyklus und (ii) die neuronale Reaktion auf den Herzschlag, sogenannte Herzschlag-evozierte Potenziale (HEP).

Zu Beginn meiner Promotion war ich Koautorin einer Verhaltensstudie, die gezeigt hat, dass die Wahrnehmbarkeit schwacher somatosensorischer Reize in der Systole geringer ist als in der Diastole. Diese Erkenntnisse motivierten die genauere Erforschung der zugrundeliegenden Mechanismen. In der Hauptstudie der Dissertation wurde an 37 gesunden Probanden der Einfluss der Herzphase sowie der HEP Amplitude auf die bewusste Wahrnehmung der Stimuli, ihre Lokalisation sowie die neuronalen Korrelate mittels Elektroencephalographie (EEG) untersucht.

Die Ergebnisse der Hauptstudie bestätigten den Unterschied in der somatosensorischen Reiz-Wahrnehmung zwischen Systole und Diastole. Mithilfe der Signalentdeckungstheorie konnten wir zeigen, dass die geringere Wahrnehmung in der Systole auf eine Veränderung der perzeptuellen Sensitivität, und nicht auf eine Verschiebung der allgemeinen Antworttendenz (Bias), zurückgeht. Ähnlich der Detektion war auch die Lokalisation während der Systole beeinträchtigt. Die verminderte Wahrnehmung in der Systole ging mit geringeren Amplituden

der späten Komponente (P300) des somatosensorisch-evozierten Potenzials (SEP) einher. Zudem waren die HEP Amplituden vor dem Reiz invers mit der somatosensorischen Detektion und Lokalisation korreliert, was auf eine Verschiebung des Entscheidungskriteriums in den konservativen Bereich zurückzuführen ist. Dieser Effekt war mit Veränderungen in frühen (P50) und späten (N140, P300) SEP-Komponenten assoziiert. Die beiden Herzschlag-bezogenen Effekte konnten nicht durch den Effekt des Alpha-Rhythmus auf die somatosensorische Wahrnehmung erklärt werden. Wir interpretieren die Herzphasen-Effekte im Rahmen eines "predictive coding"-Ansatzes und erklären die Effekte des HEP mit spontanen „Switches" zwischen Intero- und Exterozeption. In einer EEG-Folgestudie konnten wir beide Effekte replizieren.

Die zwei hier untersuchten Mechanismen der Interaktion zwischen Gehirn und Herz tragen zu einem besseren Verständnis bei, wie der Zugang zu bewusster perzeptueller Wahrnehmung reguliert wird. Im klinischen Bereich könnten analoge Herz-Hirn-Interaktionen kardiologischen Komplikationen nach Schlaganfällen sowie kognitiven Störungen im Kontext kardiologischer Erkrankungen zugrunde liegen.

1.3 Introduction

One and the same stimulus can evoke different neural responses, which is one reason why our perception of the external world, i.e., exteroception, can vary from one moment to the next. To explain the determinants of exteroception, most studies have focused on brain states[1–4] as an underlying reason for such variability in perception. However, bodily signals have been also shown to influence our cognition and behavior[5–8].

One common way of investigating body-brain interactions is by testing perception during different phases of oscillating bodily events. For example, several studies reported that conscious perception of sensory stimuli varies along the cardiac cycle[9–11]. However, studies so far have not addressed the associated psychophysical or neural mechanisms that account for such perceptual variation. Furthermore, it is unclear whether and how this effect of the cardiac phase interacts with ongoing spontaneous neural activity which is known to influence perception.

Another way of investigating body-brain interactions is by examining neural responses triggered by oscillating bodily events. For example, a growing number of studies have examined cortical

processing of cardiac signals, known as heartbeat-evoked potentials, by locking neural signals to heartbeats. Fluctuations in heartbeat-evoked potentials have been shown to affect visual perception[6]. However, whether heartbeat-evoked potentials relate to other sensory modalities and what effects they impose on upcoming sensory-evoked potentials are open questions.

This thesis presents how cardiac signals shape the perception of somatosensory stimuli and their neural processing[12]. It specifically investigates the perceptual effects of two heartbeat-related factors: (i) cardiac phase and (ii) heartbeat-evoked potentials. It examines the psychophysical mechanisms of these two heartbeat-related effects according to signal detection theory and studies the underlying neural mechanisms in an electroencephalogram (EEG) experiment using a somatosensory detection and localization task.

In the following sections of the introduction, a summary of the literature on heart-brain interactions is presented. Thereafter, the methodological approach is explained and the main findings of our work focusing on the distinct effects of these heartbeat-related events on somatosensory perception and evoked potentials are highlighted. These results are discussed in the final chapter using an integrative framework which highlights potential roles and relations between heart-brain interactions, signal detection theory, predictive coding, and the global workspace theory of consciousness.

1.3.1 Cardiac Cycle Effects on Exteroception

Cognitive processing has been suggested to be influenced differentially by the two phases of the cardiac cycle. During systole, the ventricles of the heart contract and eject blood into the arteries. During diastole, the ventricles relax and blood returns to the heart. Important to the heart and brain connection, changes in blood pressure during systole activate baroreceptors in arterial vessel walls, which leads to bursts of afferent neural activity encoding the strength and timing of individual heartbeats[13,14]. At each heartbeat, the afferent signals are first projected to the nucleus of the solitary tract (NTS) in the brainstem, then to the thalamus, and relayed up to viscerosensory cortices including the amygdala, cingulate cortex and insula[13,15–17]. Via these pathways, cardiac activity has been suggested to influence perception[5]. For example, sensory processing of external neutral stimuli has been shown to be weaker during systole compared to diastole[18–23]. These cardiac phase-dependent effects, assessed by changes in reaction time or detection performance, occur in multiple sensory modalities[18–23] (but also see [24,25] for non-

significant effect of cardiac phase). In contrast to the decreased processing of neutral stimuli, detection of fearful and threatening faces has been shown to be increased during systole compared to diastole[26]. Furthermore, more frequent microsaccades and self-initiated movements have been observed during systole[27,28]. The interoceptive predictive coding framework gives a plausible explanation to these differences in the effect of cardiac cycle on different types of stimuli. It will be discussed in further detail in section 1.3.2.

In the somatosensory domain, our research group recently demonstrated that weak somatosensory stimuli are less often detected during systole compared to diastole in a behavioral study[11]. This finding contrasts with the earlier results of Edwards et al.[29]. They reported higher somatosensory sensibility, indicated by lower detection thresholds, during systole relative to diastole. However, this discrepancy in results can be explained by a difference in methodology. Unlike in our earlier study[11], where stimulation occurred randomly across the entire cardiac cycle, they presented stimuli at three fixed time points during the cardiac cycle (Rpeak+0, Rpeak+300, Rpeak+600 ms)[29]. These stimulation time points did not cover late phases of diastole, where our previous study showed significant increases in detection[11]. Even though this likely explains the difference in the results between these two studies, further investigation in this topic is required to understand the precise effect of the cardiac phase on somatosensory perception.

Neural responses to external stimuli have also been demonstrated to vary across the cardiac cycle. In previous EEG studies, sensory-evoked responses to auditory and visual stimuli have been reported to be lower when stimuli were presented during systole as compared to diastole[10,30]. Analogously, pain-evoked potentials have also been observed to decrease during systole[31,32]. Even though these studies showed an alteration in neural responses along the cardiac cycle, they either did not examine the corresponding changes in behavior[10,30] or could not detect any behavioral changes accompanying the neural fluctuations[31–33]. Therefore, it is still unclear how exactly heartbeat-related modulations of the neural responses lead to changes in the behavioral responses.

1.3.2   Interoceptive Predictive Coding Framework

According to the predictive coding framework, the brain constructs neural representations based on previous experience. These neural representations model how sensations are generated by

stimuli[34,35]. Using these models, the brain is constantly predicting the immediate future. These predictions are based on a priori probabilities and are continuously compared with the sensory input. In this conceptual framework, the brain aims to minimize 'prediction error', which is the mismatch between its generative model and the incoming sensations[34–36].

This predictive model not only takes into account external stimuli but also interoceptive sensations such as heartbeats[34,37]. In doing so, the brain can build predictions about each heartbeat and the accompanying physiological changes in the body and it can therefore suppress them from being consciously perceived[5,34]. Thus, the brain can reduce disturbance from the rhythmic cardiac signals. When weak and neutral external stimuli coincide with these predictable cardiac events, their perception can be attenuated along with the heartbeat[5]. Supporting this view, detection of visual stimuli that are in synchrony with the heartbeat has been demonstrated to be attenuated compared to those presented asynchronously[37]. Additionally, a recent computational modelling approach proposed that suppressed integration of exteroceptive signals coincides with greater uncertainty about threatening factors in the environment[38]. Therefore, during this suppression period, the organism uses its limited resources for processing salient/fearful stimuli instead of for non-essential stimuli. This might explain previous findings that microsaccades, self-initiated movements and fear detection are increased during systole[26–28]. In short, the predictive coding framework could explain the differences in the perceptual processing of different types of stimuli along the cardiac cycle.

1.3.3 Heartbeat-Evoked Potentials

In addition to cardiac cycle effects on perception, the neural response to the heartbeat, heartbeat-evoked potential (HEP), has also been shown to influence perception. HEP can be obtained by averaging electrophysiological signals (e.g., scalp or intracranial EEG) that are time locked to heartbeats[39–41]. HEP represents the neural processing of cardiac information. They can be regarded as analogous to sensory-evoked potentials obtained by averaging EEG signals time-locked to the onset of a sensory stimulus. Importantly, however, in the case of HEP, the stimulus is internal rather than external, as is the case in sensory-evoked potentials.

Similar to sensory-evoked potentials which depend on stimulus properties (e.g., intensity) and the brain state during stimulation, HEPs are also affected by cardiac physiology and brain states[42–46]. Several studies have shown that HEP amplitudes depend on cardiac physiology such

as cardiac output, i.e., the amount of blood pumped by the heart every minute, and heart rate[42,43]. Other studies have provided evidence that the focus of attention between internal and external signals, i.e., the state of the brain at the time of the heartbeat, was accompanied by changes in HEPs[44–46]. Also, HEP amplitudes have been shown to correlate with interoceptive accuracy at a heartbeat counting task[39,40,47] and to increase through training of cardiac awareness[48].

The neural sources of HEPs in scalp and intracranial EEG studies have been previously identified in the right insula, the anterior cingulate, the prefrontal cortex, and the somatosensory cortex, which are important brain areas for interoceptive processes[41,49]. Importantly, HEP amplitudes in the precuneus and the ventromedial prefrontal cortex were shown to associate with the self-relatedness of spontaneous thoughts[50.] These two brain regions are also well regarded as hubs of the neural default-mode network (DMN), which has been implicated in several critical cognitive functions, including those that relate intimately with self-related cognition and bodily state monitoring[51]. HEPs have also been linked with bodily self-consciousness in another region of the DMN, the posterior cingulate cortex[52]. The connection of HEPs with the DMN may be due to the fact that self-related cognition often involves directing attention towards bodily signals, which lead to increases in HEPs[53]. In two other regions of the DMN, the ventromedial prefrontal cortex and right inferior parietal lobule, HEP amplitudes have also been shown to influence the detection of upcoming visual stimuli[6]. However, whether fluctuations of HEPs affect perception of external stimuli in other sensory modalities and how they affect sensory-evoked potentials are still open questions to be addressed.

1.3.4   Interoceptive Pathways from the Heart to the Brain

In the context of heart-brain interactions, it is important to mention how heartbeat-related information is relayed to the cortex and affects perception. There are four important physiological important pathways that connect the heart and the brain. First, pressure-sensitive baroreceptor activity may relay cardiac information to subcortical and cortical brain areas (as described in section 1.3.1). Second, cardiac afferent neurons in the heart wall, which are sensitive to chemical and mechanical changes, have been suggested to play a direct role in the communication between the heart and the brain. These afferent signals are transmitted to the NTS[17]. Since the NTS receives afferent information from both baroreceptors and cardiac neurons, it can integrate this information before relaying it up to viscerosensory cortices including the amygdala, cingulate cortex and insula[17]. Third, previous research has shown that

somatosensory pathways from the skin contribute to cardiac interoception[54]. Supporting the involvement of somatosensory pathways in interoception, the somatosensory cortex has been demonstrated as one of the neural sources of HEPs[41,49] and as an important area for interoception[54,55]. Finally, vascular-neuronal coupling in the central nervous system has been proposed as a potential pathway[17] since changes in blood flow have been shown to influence neural firing in rodents[56]. It is currently unclear which of these pathways is most relevant for the effects of the heart on perception[12]. Considering the importance of interoception for the body, it seems plausible that this interaction does not rely on just one but rather multiple pathways.

1.4   Objectives

This dissertation aimed to investigate the effects of dynamic coupling between the heart and the brain on somatosensory perception. In an EEG study, we investigated the effects of two heartbeat-related events on somatosensory perception and evoked potentials: i) stimulus timing along the cardiac cycle and ii) the amplitude of prestimulus HEPs.

The specific objectives of this dissertation were as follows:

- To identify the influence of cardiac phase and HEP on somatosensory detection and parameters of signal detection theory.

- To examine whether cardiac phase and HEP affect other perceptual decisions such as localizing stimulus position.

- To study whether the perceptual effects of the cardiac cycle and HEP are associated with the changes in somatosensory-evoked potentials.

- To investigate the interaction of these heartbeat-related effects with spontaneous fluctuations of alpha oscillations.

1.5   Methods

This section provides a conceptual description of the main techniques performed in this dissertation. The specific methodologies including the detailed study design, participant selection

criteria, EEG recording and preprocessing, as well as statistical analyses, are described in detail in the attached original publication[12].

1.5.1   Experimental Procedure

In the experiment, somatosensory stimuli were presented using a constant-current stimulator that generated single square-wave electrical pulses with a duration of 0.2 ms. The experiment started with the determination of a near-threshold stimulus intensity, which subjects could detect only in half of the trials, by using a two-step procedure as explained by Al et al.[12].

37 healthy subjects (20 females, age: 25.7 ± 3.9 years, range: 19 - 36 years) performed a yes/no detection and a two-alternative forced-choice (2AFC) localization task[12]. Each trial started with a presentation of a black dot on the screen for 600 ms. Afterward, subjects expected near-threshold stimulation in either their left index or middle finger. 600 ms after the stimulation, subjects answered whether they detected the stimulation by responding "yes" if they detected the stimulation and "no" if they did not detect it. Thereafter, regardless of their detection response, participants were asked to report on which finger the stimulation occurred. The next trial started immediately after answering the localization question[12]. Participants received stimulation in 800 of the 960 trials over eight experimental blocks (400 stimulations in each finger)[12]. The rest of the 160 trials did not include any stimulation, even though subjects expected there to be. After every experimental block, the stimulus intensity was readjusted to maintain the stability of the individual subject's detection threshold. (see **Fig. 1** in the study of Al et al.[12]). While participants performed the task, their EEG and electrocardiography (ECG) activity were continuously recorded.

1.5.2   Cardiac Cycle Analyses

To examine how somatosensory perception varies along the cardiac cycle, the beginning of each cardiac cycle was determined by extracting R-peaks from the ECG data[57]. Then, two complementary approaches, based on circular and binary analysis, were used to analyze perception. The following section briefly explains these approaches (for more details see the methods section described in the study of Al et al.[12]).

Circular analysis. A circular approach was used to assess somatosensory perception across the entire cardiac cycle, which allowed us to address the oscillatory aspect of cardiac activity[12,28]. Circular statistics take into account the differences in the length of the cardiac cycle between- and within-subjects[12]. Based on the relative position of the stimulation within the cardiac cycle, values between 0 and 360 degrees (0 showing the R-peak preceding stimulation) were assigned. Circular distributions of relative stimulus onsets and individual circular means were calculated for each perceptual outcome (e.g., hits, misses) in each subject individually[12]. At the group level, Rayleigh tests were applied to determine whether the distribution of stimulus onsets for each condition deviated from the uniform distribution[58].

Binary analysis. A binary approach was used to measure differences in somatosensory perception between systole and diastole. Systole was determined as the time window between the R-peak and the end of the t-wave, which was calculated using a trapezoidal area algorithm individually for each cardiac cycle[11,12,28,59]. After defining systole, its length was used to define an equal length of the diastole window at the end of each cardiac cycle (**Figure 1a**). Defining trial-specific cardiac phases has advantages over defining fixed systole and diastole windows since it takes into account the changes in the length of the cardiac phases due to within- and between-subject variations in the duration of cardiac cycle[11,12]. After defining the trial-specific systole and diastole windows, each trial was classified depending on the position of the stimulus onsets (**Figure 1b**).

1.5.3   Removal of Cardiac Artefacts

When investigating neural responses to somatosensory stimulation (i.e., SEPs) and heartbeats (i.e., HEPs), it is important to ensure that any observed effects are not contaminated by heartbeat-related artifacts such as the cardiac field artifact and/or the pulsatility artifact[41].

Cardiac Field Artifact. It is a cardiac interference generated by the strong electrical activity of the heart, which can be measured on the surface of the entire body including the scalp[41,60]. Its time-course is similar to ECG activity and it typically exhibits a strong peak coinciding with the R-peak of the ECG[41,60]. To remove the cardiac field artifact, we used an independent component analysis (ICA) approach[6,12,61]. For this purpose, we first integrated the R-peak positions as events in the EEG data and then performed an ICA using an extended infomax algorithm[61] (**Figure 1c**). Then, a copy of ICA data were epoched around the R-peak positions (-100 to 800 ms) to

determine artifactual heartbeat components that resemble the R-peak and t-wave of the ECG activity[12] by using the SASICA software (v1.3.5)[62]. After the artefactual ICA components were removed, the artifact-free components were forward-projected to sensor space in EEG.

Pulsatility Artifact. It is a cardiovascular artifact produced by micro-movements of the scalp due to blood pulsation[41]. It is commonly observed in the EEG electrodes placed near cerebral vasculature[41]. This type of artifact might be especially problematic for investigating SEPs during systole and diastole since different phases of the blood pulsation can produce artefactual differences in the SEPs. To "clean" SEPs from possible pulsatility artifacts, we developed a new technique. Briefly, random triggers were assigned along cardiac cycles and were categorized as systole and diastole according to their position in the cardiac cycle[12]. Then, data were segmented around these triggers to determine systolic and diastolic pulsatility artifact individually[12]. Finally, the average systolic and diastolic artifacts were subtracted from the SEPs during the corresponding phase of the cardiac cycle (see **Fig. S7** in the **SI Information** of Al et al.[12]).
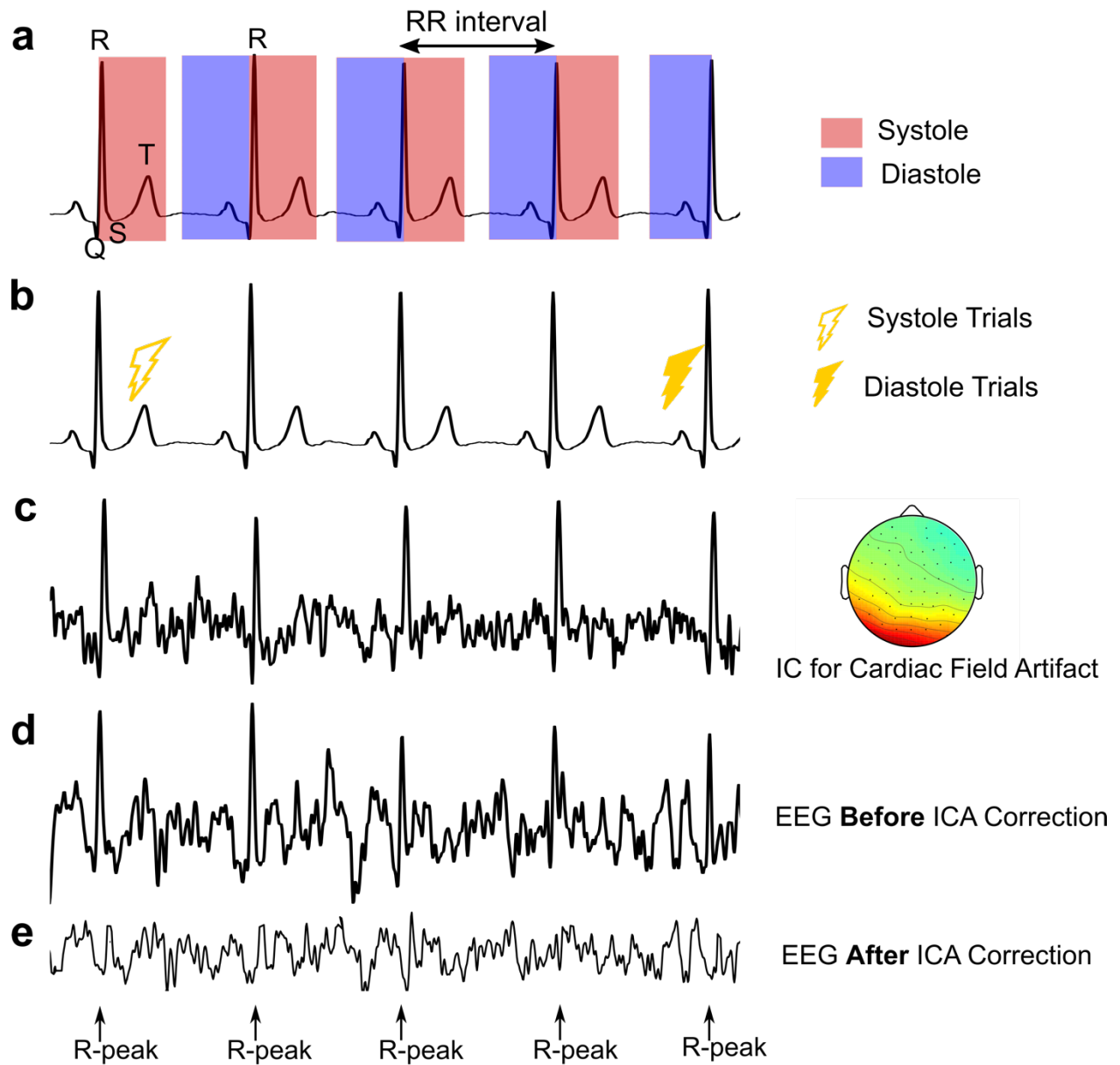
Figure 1. Cardiac activity measured by ECG and its projection in the EEG data. (**a**) An example of ECG activity in one subject. One cardiac cycle occurs in the interval between two successive R-peaks, i.e., RR interval. Trial-specific lengths of systole and diastole are calculated for every subject. Systole (red) is determined as the interval between the R-peak and the end of the T-wave. The length of this systolic window is then used to determine an equal length of diastole (blue) at the end of the cardiac cycle. (**b**) Trials are categorized depending on stimulus onset occurring during systole (open symbol) or diastole (closed symbol). (**c**) An example of an independent component (IC) representing the cardiac field artifact in the EEG data, which is determined by independent component analysis (ICA). Its time course is shown on the left and its topography on the right (d) EEG before the correction of the cardiac field artifact. (**d**) The raw EEG activity is contaminated by the cardiac field artifact. (**e**) The artifact-free EEG can be obtained by forward-projecting only artifact-free ICs into the original dataset.

1.5.4 Somatosensory-Evoked Potentials (SEPs)

After EEG preprocessing, data were segmented between -1000 and 2000 ms around the stimulus onset separately for systole and diastole trials. Then, data were baseline corrected by using the -100 to 0 ms prestimulus window. In the sensory level, the SEP analysis was done using the data from the C4 electrode since it showed the maximal P50 activity (between $40-60$ ms after stimulation) and therefore represented the contralateral primary somatosensory area[12,63,64]. The SEPs were corrected from possible cardiac artifacts by using the above-mentioned methods (for details see section 1.5.3).

1.5.5 Heartbeat-Evoked Potentials (HEPs)

Following EEG preprocessing, we calculated HEPs by epoching EEG data around the heartbeat (R-peak). We determined the time window of HEPs as $250-400$ ms following the R-peak according to the previous literature[41,47,48]. In the HEP analysis, we only included trials in which stimulation was presented "at least 400 ms after the preceding R-peak (corresponding to diastole)"[12]. In this way, HEP activity was secured against stimulation-related contaminations.

1.5.6 Time-Frequency Analyses

Time-frequency analyses were used to study prestimulus effects of sensorimotor alpha activity (between -300 and 0 ms) on perception and its possible interactions with heartbeat-related effects. An ICA-based approach was used to identify sensorimotor alpha activity, which was then validated in the source level. For every trial (epoched between $-1000-2000$ ms), a Morlet wavelet analysis was applied for frequencies between $5-40$ Hz (see further details in the Methods section of the study of Al et al.[12]).

1.5.7 Signal Detection Theory (SDT) Analyses

A 'hit' was operationally defined as a trial in which the subject detected a stimulus, a 'miss' was defined as a trial in which the subject did not detect it. A 'false alarm' (FA) was a null trial in which the subject reported feeling a stimulus. Analyses based on signal detection theory (SDT) were performed to distinguish *sensitivity* (d', the capacity to discriminate a signal from noise) and *criterion* (the tendency to report the presence or absence of the stimulus)[65,66].

In contrast to our earlier behavioral study[11], in the current study, the position of FAs could be determined across the cardiac cycle since subjects expected stimulation to always occur 600 ms after the beginning of every trial. Therefore, this study's paradigm allowed for an SDT analysis of the cardiac cycle effects.

1.5.8 Open Science Approach

The main study of the thesis aimed to follow an open science approach. Data and code were uploaded in the Open Science Framework to facilitate data and code sharing with other research groups. Due to the data protection policy of the Max Planck Institute, the link could not be shared publicly but only with scientific groups who guaranteed data privacy according to the rules of the European General Data Protection Regulation. By following this policy, the data and code were already shared with two international research groups upon their requests. Moreover, an open-access preprint of the manuscript[67] was published on bioRxiv. The final version of the manuscript was also published as open access in a peer-reviewed journal.[12]

1.5.9 Replicability of Research Findings

In recent years, the scientific community has become increasingly aware of the fact that many research findings could not be replicated ("replication crisis")[68]. It has been claimed that the majority of findings in the biomedical sciences are wrong[69]. The increasing awareness has spurred many replication studies[70]. In our lab, we take this critique serious, and therefore aim to replicate our relevant findings in independent studies. This approach is strongly reflected in this dissertation in the following ways.

My research was partially motivated by our lab's previous behavioral study[11], in which we showed decreased somatosensory detection during systole compared to diastole. This result actually differed from earlier results of Edwards et al.[29]. Even though this divergence in the results is probably explained by differences between the study designs, these differences require our scientific scrutiny. Therefore, the behavioral part of the main EEG study on phase-dependent effects replicates our earlier work. Analogously, the new findings in the main study of this thesis[12] were also tested and confirmed in a follow-up EEG study in a different cohort (Al et al., *in revision*). The latter study is available as a preprint[71].

Finally, in another behavioral study on which I collaborated with other Max Planck scientists, we tested the replicability of the cardiac cycle effects on somatosensory detection and investigated the precise relationship between the systolic suppression and pulse-related changes in the finger by using pulse oximeter (Grund et. al., *in preparation*).

In addition to the main EEG study on which this thesis is based, these replication studies (Al et al., *in revision*; Grund et. al., *in preparation*) will be briefly described in the following sections.

1.6   Results

1.6.1   Cardiac Cycle Effects on Somatosensory Perception and Evoked Potentials

Following our previous study[11], somatosensory detection was hypothesized to be lower during the early relative to later phases of the cardiac cycle. To test this hypothesis, circular and binary approaches were used. The circular analyses showed that hits across the cardiac cycle were nonuniformly distributed ($\overline{R}=0.40$, $p=0.003$) and they were more likely to occur during a later phase of the cardiac cycle (corresponding to diastole). In contrast, the nonuniform distribution of misses showed that subjects were more likely to miss stimuli during earlier phases of the cardiac cycle ($\overline{R}=0.40$, $p=0.004$)[12]. The distribution of correct localizations also demonstrated a trend toward the later phases of the cardiac cycle ($\overline{R}=0.28$, $p=0.067$). To examine cardiac cycle effects further, we used a binary approach separating the cardiac cycle into systole and diastole components. The results confirmed that somatosensory detection was significantly lower during systole (M = 49.53 %) than diastole (M = 52.41 %), $t_{36}=-3.95$, $p=3 \cdot 10^{-4}$. Decreased hit rate during systole was observed for 27 out of 37 subjects. We then investigated whether this decrease in hit rates was associated with heart rate or heart rate variability (HRV, i.e., the standard deviation of cardiac cycle durations) of participants[12]. The perceptual decrease during systole was observed to correlate with participants' HRV (Pearson's correlation, $r = -0.36$, $p = 0.03$) but not with their heart rate ($r = 0.01$, $p = 0.95$; see **Fig. S1** in the **Supplementary Information** of Al et al.[12]).

Next, we tested whether the decrease in the yes/no detection rates was associated with decreases in perceptual sensitivity (*d'*) or with adopting a more conservative criterion according to SDT. The analyses revealed that detection sensitivity was significantly lower during systole (M = 1.48)

compared to diastole, (M = 1.59; t_{36} = -2.38, p = 0.008) while no significant changes were observed for criterion (t_{36} = 0.71, p = 0.48; see **Fig. 2b** in the study of Al et al.[12]).

To connect the cardiac cycle effects with the pulse wave, which is temporally connected with heartbeats, we also investigated whether the time delay of stimulus onset from the preceding R-peak influenced detection and localization. Within-subject ANOVAs showed that detection and localization performances differed among four temporal windows: 0 – 200, 200 – 400, 400 – 600, and 600 – 800 ms following the R-peak ($F_{3,108}$ = 7.25, p = 2·10^{-4} and $F_{3,108}$ = 3.97, p = 0.01)[12]. Somatosensory detection and localization were observed to be minimum during 200–400 ms after the R-peak. (see **Fig. 2c** in the study of Al et al.[12]).

To investigate neural correlates of the cardiac phase effects on perception, we next investigated the changes in SEPs in response to stimulations during systole and diastole. A cluster-based permutation *t*-test was applied to contrast SEPs during the two cardiac phases in the time window of 0 – 600 ms following stimulus onsets over the contralateral somatosensory cortex (represented by C4 electrode). Similar to lower detection during systole, SEP amplitudes were found to be lower between 268 – 340 ms and 392 – 468 ms after stimulation during systole compared to diastole phase of the cardiac cycle (Monte Carlo p = 0.004 and p = 0.003, respectively, corrected for multiple comparisons in time; see **Fig. 3a** in Al et al.[12]). Source analysis also confirmed that the late P300 amplitude in the contralateral somatosensory cortex (S1) was significantly different between the two cardiac phases (t_{36} = -2.55, p = 0.01; see the details of source reconstruction in the **Supplementary Information** of Al et al.[12]). Furthermore, we performed exploratory analyses to investigate potential SEPs changes in other brain regions, which were previously shown to play a role in somatosensory and interoceptive processes. The investigation of right anterior insula[55], right inferior parietal lobule (rIPL)[6], bilateral anterior and posterior cingulate (ACC and PCC)[6,72], as well as bilateral lateral prefrontal cortices (LPFC)[72] revealed no significant modulation of SEPs between the two cardiac phases (see **Table S2** in the **Supplementary Information** of Al et al.[12]).

1.6.2 Effects of Heartbeat-Evoked Potentials on Somatosensory Perception and Evoked Potentials

In addition to the effects of the cardiac cycle, we also investigated the influence of prestimulus cortical responses to heartbeats, i.e., HEPs, on somatosensory detection. Prestimulus HEPs, in

the time window of 250–400 ms following the R-peak, were contrasted between hits and misses[12]. A cluster-based permutation t-test demonstrated that prestimulus HEP amplitudes between 296–400 ms following the R-peak were larger before misses compared to hits over the somatosensory and central electrodes (Monte-Carlo $p = 0.004$ corrected for multiple comparisons in space and time; see **Fig. 4a,b** in the study of Al et al.[12]).

To determine whether this perceptual effect of HEP reflected a change in sensitivity or criterion (detection bias), we performed a binning analysis. For this purpose, we sorted single trials depending on mean HEP amplitude across the cluster electrodes between 296–400 ms following R-peak and grouped them into three bins for every subject. As a result, we observed that the decrease in detection with increasing HEP amplitudes related to an increase in criterion (within-subject ANOVA, $F_{2,36} = 10.30$, $p = 1 \cdot 10^{-4}$; see **Fig. 4e** in Al et al.[12]). In other words, subjects became more conservative to report the stimulus presence as HEP amplitudes increased. Meanwhile, no significant changes in sensitivity were observed ($F_{2,72} = 0.17$, $p = 0.84$; see **Fig. 4d** in Al et al.[12]). Similar to changes in detection, correct localization rates were also observed to decrease with increasing HEP amplitudes ($F_{1.72,62.01} = 10.27$, $p = 0.03$, see **Fig. 4f** in Al et al.[12]).

We furthermore investigated the effect of prestimulus HEP levels on the upcoming SEP amplitudes. Therefore, SEP amplitudes between 0–600 ms following the stimulation were contrasted for low and high prestimulus HEP levels using a cluster-based permutation t-test. Low compared to high HEP levels were observed to be followed by higher SEP amplitudes between 32 and 600 ms after the stimulus onset over the somatosensory electrodes (Monte-Carlo $p = 0.004$ corrected for multiple comparisons in time; see **Fig. 4g** in the study of Al et al.[12]). Source reconstruction analysis also showed that the amplitude of the early SEP component, P50, was significantly differed in the contralateral primary somatosensory cortex following low and high HEP levels ($t_{36} = 2.15$, $p = 0.03$; see **Fig. S5** in the **Supplementary Information** of Al et al.[12]). We furthermore performed exploratory analyses to investigate P50 differences in other brain regions mentioned in the previous section. While a significant effect of prestimulus HEP levels on P50 amplitudes was observed after an FDR-correction in the right anterior insula ($t_{36} = 3.23$, $p = 3 \cdot 10^{-3}$), the left and right PCC ($t_{36} = -4.55$, $p = 6 \cdot 10^{-5}$ and $t_{36} = -3.39$, $p = 2 \cdot 10^{-3}$), the left and right LPFC ($t_{36} = -3.80$, $p = 5 \cdot 10^{-4}$ and $t_{36} = -4.14$, $p = 2 \cdot 10^{-4}$), no significant effect was found in the rIPL and the bilateral ACC (see **Table S3** in the **Supplementary Information** of Al et al.[12]).
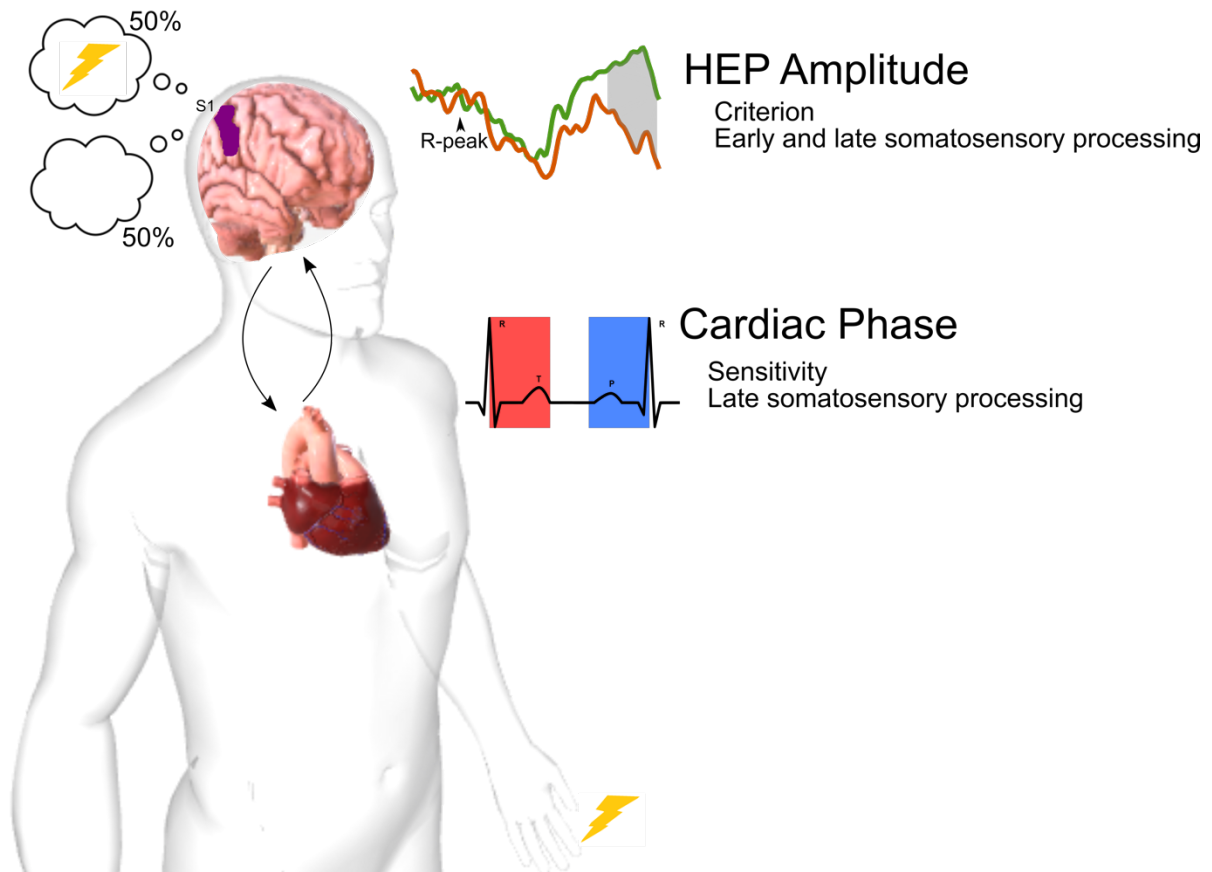
Figure 2. Effects of heart-brain interactions on somatosensory perception. The perception of a somatosensory electrical stimulus on the fingers depends on two heartbeat-related events: (i) cardiac phase that stimulation coincided with and (ii) preceding heartbeat-evoked potential (HEP) amplitudes. When a stimulus coincided with systole compared to diastole and preceded by higher HEP amplitudes, subjects are less likely to detect it. This image was created using BIODIGITAL (https://human.biodigital.com/).

1.6.3 The Independence of Cardiac Effects from Alpha Oscillations

Since prestimulus alpha oscillations have been shown to affect upcoming stimulus detection[4,73–76], we investigated alpha-related effects on somatosensory perception and a potential role of alpha oscillations in the heart and brain interactions. First, we aimed to replicate the previously shown effects of alpha on somatosensory processing[73,74]. Following previous studies[73,74], alpha amplitudes were sorted by their mean between -300 and 0 ms preceding stimulation for each trial and each subject and grouped into five equal bins. Afterward, detection and localization rates were computed for each bin. These analyses demonstrated that both detection and localization rates decreased as alpha amplitudes increased (within-subject ANOVA, $F_{2.77,99.74} = 8.88$, $p = 3 \cdot 10^{-7}$ and $F_{3.30,118.81} = 6.11$, $p = 4 \cdot 10^{-5}$; see **Fig. 5b** in the study of Al et al.[12]). This decrease in detection was mostly reflected by an increase in decision criterion (towards a more

conservative criterion; $F_{4,144} = 3.77$, $p = 0.006$; see **Fig. 5c** in Al et al.[12]). In addition to the changes in criterion, sensitivity was observed to have a trend to decrease with increasing alpha amplitudes ($F_{4,14} = 2.20$, $p = 0.07$; see **Fig. 5c** in Al et al.[12]).

Given the influence of sensorimotor alpha on somatosensory perception, we postulated that alpha oscillations might underlie the effect on perception of the cardiac cycle. We tested this hypothesis by comparing detection rates individually for systole and diastole within every alpha bin including similar alpha amplitudes for the two cardiac phases ($F_{1,36} = 0.89$, $p = 0.35$). While significant effects of cardiac phase and alpha amplitudes on detection were observed in a within-subject ANOVA test ($F_{1,36} = 15.82$, $p = 3 \cdot 10^{-4}$ and $F_{2.93,105.30} = 12.05$, $p = 1 \cdot 10^{-6}$), no significant interaction effect was found ($F_{4,144} = 0.34$, $p = 0.85$; see **Fig. 5d** in Al et al.[12]). Therefore, the cardiac phase was observed to still have an effect on stimulus detection when it was preceded by similar sensorimotor alpha levels. The independence of cardiac phase effect from the prestimulus alpha levels was also shown by using general linear mixed-effects models at a single trial level (see **Table S4** in the **Supplementary Information** of Al et al.[12]).

To gain a better understanding of the relationship between the prestimulus effects of alpha and HEP amplitudes on detection, we computed detection rates individually for low and high HEP levels within every alpha bin, including comparable alpha amplitudes for both HEP levels ($F_{1,36} = 0.14$, $p = 0.71$). While main effects of both HEP and alpha amplitude levels were observed on detection ($F_{1,36} = 38.71$, $p = 4 \cdot 10^{-7}$ and $F_{4,144} = 10.37$, $p = 2 \cdot 10^{-7}$, respectively), no interaction effect was found ($F_{4,144} = 0.75$, $p = 0.56$; see **Fig. 5e** in Al et al.[12]). This finding indicates that sensorimotor alpha and HEP amplitudes have independent influence on somatosensory detection. Supporting this result, complimentary GLMM analysis can be found in **Table S5** of the **Supplementary Information** of Al et al.[12].

1.6.4 Replication of Heartbeat-Related Perceptual Effects

As outlined above (section 1.6.1), the current study replicated our previous results showing the effect of cardiac phase on somatosensory detection and it further investigated the psychophysical and neural mechanism(s) underlying this effect. Furthermore, it showed the effects of another heartbeat-related event, which is HEP amplitude (**Figure 2**). After this study, we tested the reproducibility of these heartbeat-related effects in a follow-up EEG study using a slightly

modified detection paradigm[71] that included two temporal intervals. Only in one of them, 36 participants were presented with near-threshold electrical stimulation on their right index finger. In every trial they performed two detection tasks: a yes/no detection and a two-interval forced-choice detection task (see the details of the paradigm in the preprint of Al et al.[71]). The study also included a resting-state EEG measurement of every subject.

The results of this replication study confirmed the influence of cardiac phase and prestimulus HEP amplitudes on somatosensory perception and evoked potentials. In this study, somatosensory detection was again observed to decrease during systole relative to diastole (t_{35} = -3.41, $p = 2 \cdot 10^{-3}$)[71]. Similarly, detection correlated negatively with prestimulus HEP amplitudes between $296 - 400$ ms following the R-peak in the somatosensory and central electrodes (Monte Carlo $p = 0.001$)[71]. Correspondingly, the cardiac phase effect on detection was found to associate with changes in sensitivity (t_{35} = -3.77, $p = 6 \cdot 10^{-4}$) whereas the decrease with increasing HEP amplitudes was connected with a criterion change (within-subject ANOVA, $F_{2, 70} = 3.37$, $p = 0.04$)[71]. Moreover, the cardiac phase was again found to influence only late SEP components (Monte Carlo $p = 0.02$) while prestimulus HEP amplitudes affected both early and late SEP components (Monte-Carlo $p = 0.001$) over the contralateral somatosensory areas[71].

In addition to replicating the previous findings, there are also some new findings in this study: We observed higher HEP amplitudes when subjects were resting compared to performing an external somatosensory task (Monte-Carlo $p = 0.01$)[71]. This difference was specifically associated with a change in HEP amplitudes preceding hits ($t_{35} = 4.12$, $p = 2 \cdot 10^{-4}$) but not misses ($t_{35} = -0.04$, $p = 0.97$) during the somatosensory task[71]. Moreover, the analysis of datasets from the two studies[12,71] showed that the neural sources of HEP fluctuations preceding detection were located in two clusters of regions: one extending from the right postcentral gyrus and sulcus, the paracentral lobule and sulcus to the superior parietal lobule and another extending across the right precuneus, pericallosal sulcus, isthmus cingulate, middle and posterior cingulate cortex (see **Fig. 4** in the preprint of Al et al.[71]). In these regions, HEP amplitudes were similar to those during the resting-state (see **Fig. 5** in the preprint of Al et al.[71]).

The last behavioral experiment included a somatosensory yes/no detection task that was followed up by confidence ratings of subjects for their detection responses. Meanwhile, subjects' respiratory and cardiac activity as well as blood pulse in the fingers were measured. Our

preliminary results confirm the systolic suppression of somatosensory detection and suggest that subjects' detection was minimal when stimulus occurred between $250-300$ ms after the R-peak, when the blood pressure in the finger is initially starting to rise (Grund et. al., *in preparation*).

1.7   Discussion

1.7.1   Heartbeat-Related Effects on Somatosensory Perception

The main findings[12] are that (i) cardiac phase and (ii) prestimulus HEP amplitudes differentially affect somatosensory perception and evoked potentials. Specifically, (i) somatosensory stimuli were less often detected during systole as compared to diastole and higher prestimulus HEP amplitudes were associated with less detection While cardiac phase modulated mainly sensitivity of stimulus detection, fluctuations of the HEP amplitude went along with criterion changes. Furthermore, cardiac phase had effects on only late SEP components (P300) whereas prestimulus HEP amplitudes influenced both early (P50) and later components (N140, P300). These two heartbeat-related perceptual effects were independent and additive to the influence of sensorimotor background (alpha) oscillations on somatosensory perception.

The effect of cardiac phase on perception and neural activity seems best interpreted in an interoceptive predictive framework (see section 1.3.2 for more details). According to this framework, the brain forms predictions regarding each heartbeat and its concurrent pulse wave (e.g., through baroreceptor activity), which causes temporary physiological changes in the body[5,34]. Depending on these predictions, the brain can suppress the recurring cardiac afferent signals from being consciously perceived. Thus, interference from internal signals, e.g., pulse-related changes, can be attenuated[34,35]. Supporting this interpretation for the somatosensory system, afferent neurons in the fingers have been demonstrated to fire in response to the pulse wave[77] that reaches a maximal pressure around 200 to 400 ms after the R-peak during systole[12,78]. Even though this neuronal activity is strong enough to reach perceptual levels, the ongoing pulsations are not perceived in the fingers because these heartbeat-coupled changes are probably predicted and attenuated by the central processes[12,77].

Since detection was smallest when stimulus was presented within 200 to 400 ms after the R-peak, we propose that the same predictive mechanism suppressing the heartbeat-related events can also attenuate the perception of a weak somatosensory stimulus during systole coinciding

with the changes in the pulse-wave. This prediction may be also influenced by the sequence of previous heartbeats, as the present data indicate that perceptual attenuation was stronger in individuals who had less heart rate variability (HRV). It should be added that this latter effect was not replicated in a follow-up study[71]. Furthermore, the systolic attenuation of detection was associated with a decrease in sensitivity. In other words, it was harder to distinguish a weak stimulus from "noise" during systole since it was more often considered as part of the "internal noise" of the body[12]. Supporting this finding, correctly localizing a stimulus on a finger was also harder during systole.

In line with the attenuation of somatosensory perception, the late P300 component of SEPs was suppressed during systole compared to diastole. Such decrease in P300 amplitude has been connected with a smaller 'prediction error'[79] and therefore its decrease during systole might indicate a more precise prediction of the pulse-wave. Therefore, P300 attenuation during systole can be interpreted as the outcome of a prediction mechanism in the brain which can suppress perception of peripheral pulse activity[12]. Furthermore, conscious detection of a stimulus has often been observed to correlate with P300 amplitudes[80–82]. The reduction of both P300 amplitude and somatosensory sensitivity during systole might be associated with a less efficient propagation of neural activity to higher cortical areas[12,83]. According to the global neural workspace theory, a decline in neural propagation can impede the global 'broadcasting' of the stimulus and thus prevent conscious perception of the somatosensory stimulus[79,82].

In addition to the effects of the cardiac phase on somatosensory processing, prestimulus HEP amplitudes were observed to influence somatosensory detection. We found decreases in somatosensory detection and localization following higher HEP amplitudes between 296 to 400 ms (after the R-peak) over centroparietal electrodes[12]. Lower stimulus detection with higher HEP amplitudes were associated with an adaptation of a more conservative detection criterion (bias)[12]. As a conservative bias has been connected with lower baseline firing in the brain (cortical excitability), higher prestimulus HEP amplitudes might impede somatosensory detection by blocking early neural activity to reach the threshold for 'ignition'[82,83].

Supporting this view, higher HEP amplitudes were observed to interfere with both early (P50) and late (N140, P300) SEP components at the sensory level. Spatially, HEP amplitudes correlated significantly with source-localized P50 amplitudes in the contralateral somatosensory cortex, right insular cortex, lateral prefrontal cortex, and posterior cingulate cortex[12]. The right

anterior insula is often referred as an 'integral hub' that regulates attention internally and externally[55], perhaps through its connections with the two other regions playing a role in attentional control, the lateral prefrontal cortex and the posterior cingulate cortex[84]. Correspondingly, P50 amplitudes have been previously reported to depend on spatial attention[73,85]. Given previous studies have shown that HEP amplitudes increase when attention is oriented internally relative to externally[44–46], higher HEP amplitudes preceding misses may indicate an attentional shift from exteroceptive stimuli to interoceptive bodily signals[86].

While we observed a negative relationship between prestimulus HEP amplitude and stimulus detection, in the visual domain an opposite pattern has been observed: In a magnetoencephalography (MEG) study, Park et al.[6] have previously shown that higher HEP amplitudes were followed by increased detection of a visual stimulus. These contradictory results might be due to differences in the involvement of somatosensory and visual cortices in the processing of interoceptive signals[12]. For instance, during a higher interoceptive state, a previous study showed that the anterior insula, an important area for interoception, showed a higher coupling with the somatosensory cortex but a lower coupling with the visual cortex[87]. As explained earlier (see above 1.3.4), somatosensory pathways from the skin have been shown to contribute to cardiac interoception[54]. The somatosensory cortex has also been shown to be one of the neural sources of HEPs[41,49] and a significant area for interoception[54,55]. Given the essential role of the somatosensory cortex for interoception, the processing of somatosensory but not visual stimuli may likely interfere with interoceptive processes and therefore with HEP amplitudes[12].

Finally, we investigated how heartbeat-related effects are connected with ongoing sensorimotor oscillations. In line with previous research, we first confirmed the effect of prestimulus sensorimotor alpha oscillations on somatosensory perception[75,89,90]. Specifically, our results showed that higher levels of prestimulus alpha amplitude were followed by decreases in somatosensory detection, which was associated with a more conservative detection criterion. Similar effects of alpha amplitude have been previously shown for visual[73] and somatosensory[90] detection. In addition to detection, somatosensory localization was also observed to decrease with increasing prestimulus alpha amplitudes. Since sensorimotor alpha amplitudes were observed to influence somatosensory perception, we further investigated whether alpha oscillations were responsible for the observed heartbeat-related effects. Our findings demonstrated that neither the cardiac phase- nor HEP-related effects on perception were

dependent on prestimulus alpha amplitudes, rather these heartbeat-related effects were additive to the influence of prestimulus sensorimotor alpha amplitude on detection[12].

1.7.2 Cardiac Health and Interoceptive Wellness

Understanding heart-brain interactions is likely to be relevant for our health since disruptions of interoceptive processes have been shown in different clinical conditions such as anxiety disorders and depression[91,92]. Pathological heart-brain interactions probably also underly the observation that severe cardiac complications often occur after a stroke[93]. Moreover, abnormalities in cardiac function can both exacerbate preexisting brain damage and trigger new brain injury[93]. Thus, future clinical studies might benefit from assessing "biomarkers" of heart-brain interactions such as HEP amplitudes to better understand abnormalities in heart-brain interactions in patients with psychiatric and neurological disorders.

1.7.3 Limitations of the Current Study

The main EEG study has several limitations: First, this study did not include a measure of blood pressure in the fingers. Even though it is possible to infer the time window of pulse-related changes in the fingers from ECG measurements, it is only an approximation. For example, the perceptual suppression during systole might coincide the initial or maximal changes in blood pressure. This cannot be concluded from the present study[12]. To answer this question, in an additional study, my collaborators and I measured blood pressure in the fingers using a pulse oximeter together with ECG (Grund et. al., *in preparation*).

Second, the current EEG study did not include a direct measure of attention. Since we did not induce any systematic changes in attention to external or internal events, we assumed the fluctuations of HEP to be spontaneous, reflecting changes in interoception and exteroception[44–46]. Therefore, in addition to a somatosensory task, in a follow-up study[71] (see above 1.3.5), we introduced a resting-state condition in which exteroceptive attention is expected to be minimal in opposition to the task condition, where subjects were asked to attend to an external somatosensory stimulus.

Third, even though the current results confirm the important role of the somatosensory cortex for interoceptive processes, it is not clear how the somatosensory cortex is connected with other interoceptive areas such as the cingulate cortex and insula. The connectivity patterns of

somatosensory cortex with the other interoceptive regions during exteroception and interoception can be examined in future studies.

Fourth, this thesis showed the effects of the cardiac phase and HEP amplitudes on somatosensory perception. While one possible interpretation of the findings is a modulation of global cortical excitability, our study did not specifically address how these two heartbeat-related factors are connected with overall cortical excitability levels. To study the relationship between these effects and motor excitability levels, we conducted another study by combining EEG, ECG, and transcranial magnetic stimulation (TMS) techniques. In this study, we will specifically analyze motor-evoked potentials, which are measured in response to TMS stimulation over the primary motor cortex, as a marker of motor excitability levels. This TMS-EEG study will answer whether motor excitability change across the cardiac cycle (Al et al., *in preparation*).

1.7.4 Replicability of the Heartbeat-Related Effects on Somatosensory Perception

Confirming the results of an earlier behavioral study that I coauthored[11], the current study first replicated the cardiac phase effect on somatosensory detection and then investigated psychophysical and neural mechanisms of this effect along with the influence of HEP amplitudes.

In a follow-up EEG study with a slightly modified detection paradigm[71], we replicated the impact of cardiac phase and prestimulus HEP amplitudes on somatosensory perception and evoked potentials. Additionally, new results located the neural sources of HEP fluctuations preceding detection in two clusters of regions: one extending from the right postcentral gyrus and sulcus, the paracentral lobule and sulcus to the superior parietal lobule and another extending across the right precuneus, pericallosal sulcus, isthmus cingulate, middle and posterior cingulate cortex[71]. Among these brain areas, the paracentral lobule, the postcentral gyrus, middle and posterior cingulate cortex, and precuneus have been previously shown to be highly activated during an interoceptive relative to exteroceptive task and to associate with interoceptive awareness[71,94]. Given that HEP fluctuations preceding detection were associated with brain areas that are known to be involved in interoceptive processing, higher HEP amplitudes are likely to indicate a state of mind attending to internal bodily processes[71]. Supporting the mechanism of HEP amplitudes increases when attention turns inwardly higher HEP amplitudes were observed when subjects were resting compared to performing an external somatosensory task. This

difference was specifically connected with a change in HEP amplitudes preceding hits but not misses[71]. Therefore, these findings not only confirm the results of the current thesis but also strengthen the proposed conceptual interpretation regarding heartbeat-related effects on perception.

Preliminary results from another behavioral experiment confirmed that somatosensory detection is lower during systole relative to diastole. This study furthermore looked at the precise timing of the cardiac phase effects with respective to the pulse wave in the finger and showed that the systolic suppression coincides with the initial changes of the finger blood pressure during systole, rather than with its maximum. Thus, somatosensory perception in the fingers might be suppressed specifically during the initial rise of the finger pulse (Grund et. al., *in preparation*).

1.7.5   Conclusion

My doctoral thesis presented here shows that cardiac phase and HEP amplitudes shape conscious perception of weak somatosensory stimuli differentially through the mediation of distinct neural processes. We explain the effects of cardiac phase in the framework of interoceptive predictive coding and propose the HEP effects to be connected with spontaneous attentional shifts between interoception and exteroception. These results thus contribute to our knowledge of how internal bodily signals can influence conscious perception of the external world.

1.8 Bibliography

1. Arieli, A., Sterkin, A., Grinvald, A. & Aertsen, A. Dynamics of ongoing activity: explanation of the large variability in evoked cortical responses. *Science* **273,** 1868–71 (1996).

2. Weisz, N., Wuhle, A., Monittola, G., Demarchi, G., Frey, J., Popov, T. & Braun, C. Prestimulus oscillatory power and connectivity patterns predispose conscious somatosensory perception. *Proc. Natl. Acad. Sci.* **111,** E417–E425 (2014).

3. Gelbard-Sagiv, H., Mudrik, L., Hill, M. R., Koch, C. & Fried, I. Human single neuron activity precedes emergence of conscious perception. *Nat. Commun.* **9,** 2057 (2018).

4. van Dijk, H., Schoffelen, J.-M., Oostenveld, R. & Jensen, O. Prestimulus Oscillatory Activity in the Alpha Band Predicts Visual Discrimination Ability. *J. Neurosci.* **28,** 1816–1823 (2008).

5. Critchley, H. D. & Garfinkel, S. N. The influence of physiological signals on cognition. *Curr. Opin. Behav. Sci.* **19,** 13–18 (2018).

6. Park, H.-D., Correia, S., Ducorps, A. & Tallon-Baudry, C. Spontaneous fluctuations in neural responses to heartbeats predict visual detection. *Nat. Neurosci.* **17,** 612–618 (2014).

7. Craig, A. D. How do you feel - now? The anterior insula and human awareness. *Nat. Rev. Neurosci.* **10,** 59–70 (2009).

8. Gallagher, S. *How the body shapes the mind*. (Clarendon Press, 2006).

9. Saxon, S. A. Detection of near threshold signals during four phases of cardiac cycle. *Ala. J. Med. Sci.* **7,** 427–30 (1970).

10. Sandman, C. A. Augmentation of the auditory event related potentials of the brain during diastole. *Int. J. Psychophysiol.* **2,** 111–119 (1984).

11. Motyka, P., Grund, M., Forschack, N., Al, E., Villringer, A. & Gaebler, M. Interactions between cardiac activity and conscious somatosensory perception. *Psychophysiology* e13424 (2019).

12. Al, E., Iliopoulos, F., Forschack, N., Nierhaus, T., Grund, M., Motyka, P., Gaebler, M., Nikulin, V. V. & Villringer, A. Heart-brain interactions shape somatosensory perception and evoked potentials. *Proc. Natl. Acad. Sci. U. S. A.* **117,** 10575–10584 (2020).

13. Critchley, H. D. & Harrison, N. A. Visceral Influences on Brain and Behavior. *Neuron* **77,** 624–638 (2013).

14. Azevedo, R. T., Garfinkel, S. N., Critchley, H. D. & Tsakiris, M. Cardiac afferent activity modulates the expression of racial stereotypes. *Nat. Commun.* **8,** 1–9 (2017).

15. Zhang, Z. H., Dougherty, P. M. & Oppenheimer, S. M. Monkey insular cortex neurons respond to baroreceptive and somatosensory convergent inputs. *Neuroscience* **94,** 351–360 (1999).

16. Dampney, R. A. L. Central neural control of the cardiovascular system: current perspectives. *Adv. Physiol. Educ.* **40,** 283–296 (2016).

17. Park, H.-D. & Blanke, O. Heartbeat-evoked cortical responses: Underlying mechanisms, functional roles, and methodological considerations. *Neuroimage* **197,** 502–511 (2019).

18. Birren, J. E., Cardon, P. V. & Phillips, S. L. Reaction time as a function of the cardiac cycle in young adults. *Science* **140,** 195–196 (1963).

19. Edwards, L., Ring, C., McIntyre, D., Carroll, D. & Martin, U. Psychomotor speed in hypertension: Effects of reaction time components, stimulus modality, and phase of the cardiac cycle. *Psychophysiology* **44,** 459–468 (2007).

20. McIntyre, D., Ring, C., Edwards, L. & Carroll, D. Simple reaction time as a function of the phase of the cardiac cycle in young adults at risk for hypertension. *Psychophysiology* **45,** 333–336 (2008).

21. Saari, M. J. & Pappas, B. A. Cardiac Cycle Phase and Movement and Reaction Times. *Percept. Mot. Skills* **42,** 767–770 (1976).

22. Sandman, C. A., McCanne, T. R., Kaiser, D. N. & Diamond, B. Heart rate and cardiac phase influences on visual perception. *J. Comp. Physiol. Psychol.* **91,** 189–202 (1977).

23. Wilkinson, M., McIntyre, D. & Edwards, L. Electrocutaneous pain thresholds are higher during systole than diastole. *Biol. Psychol.* **94,** 71–73 (2013).

24. Elliott, R. & Graf, V. Visual Sensitivity as a Function of Phase of Cardiac Cycle. *Psychophysiology* **9,** 357–361 (1972).

25. Delfini, L. F. & Campos, J. J. Signal Detection and the 'Cardiac Arousal Cycle'. *Psychophysiology* **9,** 484–491 (1972).

26. Garfinkel, S. N., Minati, L., Gray, M. A., Seth, A. K., Dolan, R. J. & Critchley, H. D. Fear from the heart: Sensitivity to fear stimuli depends on individual heartbeats. *J. Neurosci.* **34,** 6573–6582 (2014).

27. Ohl, S., Wohltat, C., Kliegl, R., Pollatos, O. & Engbert, R. Microsaccades are coupled to heartbeat. *J. Neurosci.* **36,** 1237–1241 (2016).

28. Kunzendorf, S., Klotzsche, F., Akbal, M., Villringer, A., Ohl, S. & Gaebler, M. Active information sampling varies across the cardiac cycle. *Psychophysiology* **56,** 1–16 (2019).

29. Edwards, L., Ring, C., Mcintyre, D., Winer, J. & Martin, U. Sensory detection thresholds are modulated across the cardiac cycle: Evidence that cutaneous sensibility is greatest for

systolic stimulation. *Psychophysiology* **46,** 252–256 (2009).

30. Walker, B. B. & Sandman, C. A. Visual Evoked Potentials Change as Heart Rate and Carotid Pressure Change. *Psychophysiology* **19,** 520–527 (1982).

31. Gray, M. A., Minati, L., Paoletti, G. & Critchley, H. D. Baroreceptor activation attenuates attentional effects on pain-evoked potentials. *Pain* **151,** 853–61 (2010).

32. Edwards, L., Inui, K., Ring, C., Wang, X. & Kakigi, R. Pain-related evoked potentials are modulated across the cardiac cycle. *PAIN®* **137,** 488–494 (2008).

33. Park, H.-D. & Tallon-Baudry, C. The neural subjective frame: from bodily signals to perceptual consciousness. *Philos. Trans. R. Soc. B Biol. Sci.* **369,** 20130208 (2014).

34. Barrett, L. F. & Simmons, W. K. Interoceptive predictions in the brain. *Nat. Rev. Neurosci.* **16,** 419–429 (2015).

35. Seth, A. K. & Friston, K. J. Active interoceptive inference and the emotional brain. *Philos. Trans. R. Soc. B Biol. Sci.* **371,** (2016).

36. Friston, K., Kilner, J. & Harrison, L. A free energy principle for the brain. *J. Physiol.* **100,** 70–87 (2006).

37. Salomon, R., Ronchi, R., Dönz, J., Bello-Ruiz, J., Herbelin, B., Martet, R., Faivre, N., Schaller, K. & Blanke, O. The Insula Mediates Access to Awareness of Visual Stimuli Presented Synchronously to the Heartbeat. *J. Neurosci.* **36,** 5115–5127 (2016).

38. Allen, M., Levy, A., Parr, T. & Friston, K. J. In the Body's Eye: The Computational Anatomy of Interoceptive Inference. *bioRxiv* 603928 (2019). doi:10.1101/603928

39. Montoya, P., Schandry, R. & Müller, A. Heartbeat evoked potentials (HEP): topography and influence of cardiac awareness and focus of attention. *Electroencephalogr. Clin. Neurophysiol. Potentials Sect.* **88,** 163–172 (1993).

40. Pollatos, O. & Schandry, R. Accuracy of heartbeat perception is reflected in the amplitude of the heartbeat-evoked brain potential. *Psychophysiology* **41,** 476–82 (2004).

41. Kern, M., Aertsen, A., Schulze-Bonhage, A. & Ball, T. Heart cycle-related effects on event-related potentials, spectral power changes, and connectivity patterns in the human ECoG. *Neuroimage* **81,** 178–190 (2013).

42. Gray, M. A., Taggart, P., Sutton, P. M., Groves, D., Holdright, D. R., Bradbury, D., Brull, D. & Critchley, H. D. A cortical potential reflecting cardiac function. *Proc. Natl. Acad. Sci.* **104,** 6818 LP – 6823 (2007).

43. Schandry, R. & Montoya, P. Event-related brain potentials and the processing of cardiac activity. *Biol. Psychol.* **42,** 75–85 (1996).

44. Villena-González, M., Moënne-Loccoz, C., Lagos, R. A., Alliende, L. M., Billeke, P.,

Aboitiz, F., López, V. & Cosmelli, D. Attending to the heart is associated with posterior alpha band increase and a reduction in sensitivity to concurrent visual stimuli. *Psychophysiology* **54,** 1483–1497 (2017).

45. García-Cordero, I., Esteves, S., Mikulan, E. P., Hesse, E., Baglivo, F. H., Silva, W., García, M. D. C., Vaucheret, E., Ciraolo, C., García, H. S., Adolfi, F., Pietto, M., Herrera, E., Legaz, A., Manes, F., García, A. M., Sigman, M., Bekinschtein, T. A., Ibáñez, A. & Sedeño, L. Attention, in and Out: Scalp-Level and Intracranial EEG Correlates of Interoception and Exteroception. *Front. Neurosci.* **11,** 411 (2017).

46. Petzschner, F. H., Weber, L. A., Wellstein, K. V., Paolini, G., Do, C. T. & Stephan, K. E. Focus of attention modulates the heartbeat evoked potential. *Neuroimage* **186,** 595–606 (2019).

47. Schandry, R., Sparrer, B. & Weitkunat, R. From the heart to the brain: a study of heartbeat contingent scalp potentials. *Int. J. Neurosci.* **30,** 261–75 (1986).

48. Schandry, R. & Weitkunat, R. Enhancement of heartbeat-related brain potentials through cardiac awareness training. *Int. J. Neurosci.* **53,** 243–53 (1990).

49. Pollatos, O., Kirsch, W. & Schandry, R. Brain structures involved in interoceptive awareness and cardioafferent signal processing: A dipole source localization study. *Hum. Brain Mapp.* **26,** 54–64 (2005).

50. Babo-Rebelo, M., Richter, C. G. & Tallon-Baudry, C. Neural responses to heartbeats in the default network encode the self in spontaneous thoughts. *J. Neurosci.* **36,** 7829–7840 (2016).

51. Raichle, M. E., MacLeod, A. M., Snyder, A. Z., Powers, W. J., Gusnard, D. A. & Shulman, G. L. A default mode of brain function. *Proc. Natl. Acad. Sci. U. S. A.* **98,** 676–682 (2001).

52. Park, X. H.-D., Bernasconi, F., Bello-Ruiz, J., Pfeiffer, C., Salomon, R. & Blanke, O. Transient Modulations of Neural Responses to Heartbeats Covary with Bodily Self-Consciousness. (2016). doi:10.1523/JNEUROSCI.0311-16.2016

53. Azzalini, D., Rebollo, I. & Tallon-Baudry, C. Visceral Signals Shape Brain Dynamics and Cognition. *Trends Cogn. Sci.* **23,** 488–509 (2019).

54. Khalsa, S. S., Rudrauf, D., Feinstein, J. S. & Tranel, D. The pathways of interoceptive awareness. *Nat. Neurosci.* **12,** 1494–6 (2009).

55. Critchley, H. D., Wiens, S., Rotshtein, P., Öhman, A. & Dolan, R. J. Neural systems supporting interoceptive awareness. *Nat. Neurosci.* **7,** 189–195 (2004).

56. Kim, K. J., Diaz, J. R., Iddings, J. A. & Filosa, J. A. Vasculo-neuronal coupling:

Retrograde vascular communication to brain neurons. *J. Neurosci.* **36,** 12624–12639 (2016).

57. Tarvainen, M. P., Niskanen, J.-P., Lipponen, J. A., Ranta-aho, P. O. & Karjalainen, P. A. Kubios HRV – Heart rate variability analysis software. *Comput. Methods Programs Biomed.* **113,** 210–220 (2014).

58. Pewsey, A., Neuhäuser, M. & Ruxton, G. *Circular statistics in R*. (2013).

59. Vázquez-Seisdedos, C. R., Neto, J. E., Marañón Reyes, E. J., Klautau, A. & Limão de Oliveira, R. C. New approach for T-wave end detection on electrocardiogram: performance in noisy conditions. *Biomed. Eng. Online* **10,** 77 (2011).

60. Dirlich, G., Vogl, L., Plaschke, M. & Strian, F. *Cardiac field effects on the EEG. Electroencephalogr. Clin. Neurophysiol.* **102,** (1997).

61. Delorme, A., Palmer, J., Onton, J., Oostenveld, R. & Makeig, S. Independent EEG Sources Are Dipolar. *PLoS One* **7,** e30135 (2012).

62. Chaumon, M., Bishop, D. V. M. & Busch, N. A. A practical guide to the selection of independent components of the electroencephalogram for artifact correction. *J. Neurosci. Methods* **250,** 47–63 (2015).

63. Zhang, Y. & Ding, M. Detection of a weak somatosensory stimulus: Role of the prestimulus mu rhythm and its top-down modulation. *J. Cogn. Neurosci.* **22,** 307–322 (2010).

64. Nierhaus, T., Forschack, N., Piper, S. K., Holtze, S., Krause, T., Taskin, B., Long, X., Stelzer, J., Margulies, D. S., Steinbrink, J. & Villringer, A. Imperceptible somatosensory stimulation alters sensorimotor background rhythm and connectivity. *J. Neurosci.* **35,** 5917–25 (2015).

65. Macmillan, N. & Creelman, D. *Detection Theory: A User's Guide. Detect. Theory A User's Guid. 2nd Ed.* (2004). doi:10.4324/9781410611147

66. Green, D. M. & Swets, J. A. Signal detection theory and psychophysics. **1,** (1966).

67. Al, E., Iliopoulos, F., Forschack, N., Nierhaus, T., Grund, M., Motyka, P., Gaebler, M., Nikulin, V. V. & Villringer, A. Heart-brain interactions shape somatosensory perception and evoked potentials. *bioRxiv* 750315 (2019). doi:10.1101/750315

68. Tackett, J. L., Brandes, C. M., King, K. M. & Markon, K. E. Psychology's Replication Crisis and Clinical Psychological Science. *Annu. Rev. Clin. Psychol.* **15,** 579–604 (2019).

69. Ioannidis, J. P. A. Why Most Published Research Findings Are False. *PLoS Med.* **2,** e124 (2005).

70. Botvinik-Nezer, R., Holzmeister, F., Camerer, C. F., Dreber, A., Huber, J., Johannesson,

M., Kirchler, M., Iwanir, R., Mumford, J. A., Adcock, R. A., Avesani, P., Baczkowski, B. M., Bajracharya, A., Bakst, L., Ball, S., Barilari, M., Bault, N., Beaton, D., Beitner, J., Benoit, R. G., Berkers, R. M. W. J., Bhanji, J. P., Biswal, B. B., Bobadilla-Suarez, S., Bortolini, T., Bottenhorn, K. L., Bowring, A., Braem, S., Brooks, H. R., Brudner, E. G., Calderon, C. B., Camilleri, J. A., Castrellon, J. J., Cecchetti, L., Cieslik, E. C., Cole, Z. J., Collignon, O., Cox, R. W., Cunningham, W. A., Czoschke, S., Dadi, K., Davis, C. P., Luca, A. De, Delgado, M. R., Demetriou, L., Dennison, J. B., Di, X., Dickie, E. W., Dobryakova, E., Donnat, C. L., Dukart, J., Duncan, N. W., Durnez, J., Eed, A., Eickhoff, S. B., Erhart, A., Fontanesi, L., Fricke, G. M., Fu, S., Galván, A., Gau, R., Genon, S., Glatard, T., Glerean, E., Goeman, J. J., Golowin, S. A. E., González-García, C., Gorgolewski, K. J., Grady, C. L., Green, M. A., Guassi Moreira, J. F., Guest, O., Hakimi, S., Hamilton, J. P., Hancock, R., Handjaras, G., Harry, B. B., Hawco, C., Herholz, P., Herman, G., Heunis, S., Hoffstaedter, F., Hogeveen, J., Holmes, S., Hu, C. P., Huettel, S. A., Hughes, M. E., Iacovella, V., Iordan, A. D., Isager, P. M., Isik, A. I., Jahn, A., Johnson, M. R., Johnstone, T., Joseph, M. J. E., Juliano, A. C., Kable, J. W., Kassinopoulos, M., Koba, C., Kong, X. Z., Koscik, T. R., Kucukboyaci, N. E., Kuhl, B. A., Kupek, S., Laird, A. R., Lamm, C., Langner, R., Lauharatanahirun, N., Lee, H., Lee, S., Leemans, A., Leo, A., Lesage, E., Li, F., Li, M. Y. C., Lim, P. C., Lintz, E. N., Liphardt, S. W., Losecaat Vermeer, A. B., Love, B. C., Mack, M. L., Malpica, N., Marins, T., Maumet, C., McDonald, K., McGuire, J. T., Melero, H., Méndez Leal, A. S., Meyer, B., Meyer, K. N., Mihai, G., Mitsis, G. D., Moll, J., Nielson, D. M., Nilsonne, G., Notter, M. P., Olivetti, E., Onicas, A. I., Papale, P., Patil, K. R., Peelle, J. E., Pérez, A., Pischedda, D., Poline, J. B., Prystauka, Y., Ray, S., Reuter-Lorenz, P. A., Reynolds, R. C., Ricciardi, E., Rieck, J. R., Rodriguez-Thompson, A. M., Romyn, A., Salo, T., Samanez-Larkin, G. R., Sanz-Morales, E., Schlichting, M. L., Schultz, D. H., Shen, Q., Sheridan, M. A., Silvers, J. A., Skagerlund, K., Smith, A., Smith, D. V., Sokol-Hessner, P., Steinkamp, S. R., Tashjian, S. M., Thirion, B., Thorp, J. N., Tinghög, G., Tisdall, L., Tompson, S. H., Toro-Serey, C., Torre Tresols, J. J., Tozzi, L., Truong, V., Turella, L., van 't Veer, A. E., Verguts, T., Vettel, J. M., Vijayarajah, S., Vo, K., Wall, M. B., Weeda, W. D., Weis, S., White, D. J., Wisniewski, D., Xifra-Porxas, A., Yearling, E. A., Yoon, S., Yuan, R., Yuen, K. S. L., Zhang, L., Zhang, X., Zosky, J. E., Nichols, T. E., Poldrack, R. A. & Schonberg, T. Variability in the analysis of a single neuroimaging dataset by many teams. *Nature* **582,** 84–88 (2020).

71.   Al, E., Iliopoulos, F., Nikulin, V. V & Villringer, A. Heartbeat and Somatosensory

Perception. *bioRxiv* 2020.12.29.424693 (2020). doi:10.1101/2020.12.29.424693

72. Hirvonen, J. & Palva, S. Cortical localization of phase and amplitude dynamics predicting access to somatosensory awareness. *Hum. Brain Mapp.* **37,** 311–326 (2016).

73. Iemi, L., Chaumon, M., Crouzet, S. M. & Busch, N. A. Spontaneous Neural Oscillations Bias Perception by Modulating Baseline Excitability. *J. Neurosci.* **37,** 807–819 (2017).

74. Forschack, N., Nierhaus, T., Müller, M. M. & Villringer, A. Alpha-Band Brain Oscillations Shape the Processing of Perceptible as well as Imperceptible Somatosensory Stimuli during Selective Attention. *J. Neurosci.* **37,** 6983–6994 (2017).

75. Schubert, R., Haufe, S., Blankenburg, F., Villringer, A. & Curio, G. Now You'll Feel It, Now You Won't: EEG Rhythms Predict the Effectiveness of Perceptual Masking. *J. Cogn. Neurosci.* **21,** 2407–2419 (2009).

76. Haegens, S., Nácher, V., Luna, R., Romo, R. & Jensen, O. α-Oscillations in the monkey sensorimotor network influence discrimination performance by rhythmical inhibition of neuronal spiking. *Proc. Natl. Acad. Sci. U. S. A.* **108,** 19377–82 (2011).

77. Macefield, V. G. Cardiovascular and respiratory modulation of tactile afferents in the human finger pad. *Exp. Physiol.* **88,** 617–25 (2003).

78. van Velzen, M. H. N., Loeve, A. J., Niehof, S. P. & Mik, E. G. Increasing accuracy of pulse transit time measurements by automated elimination of distorted photoplethysmography waves. *Med. Biol. Eng. Comput.* **55,** 1989–2000 (2017).

79. Friston, K. A theory of cortical responses. *Philos. Trans. R. Soc. B Biol. Sci.* **360,** 815–836 (2005).

80. Dehaene, S., Sergent, C. & Changeux, J.-P. A neuronal network model linking subjective reports and objective physiological data during conscious perception. *Proc. Natl. Acad. Sci.* **100,** 8520–8525 (2003).

81. Lamme, V. A. F. Towards a true neural stance on consciousness. *Trends Cogn. Sci.* **10,** 494–501 (2006).

82. Auksztulewicz, R., Spitzer, B. & Blankenburg, F. Recurrent neural processing and somatosensory awareness. *J. Neurosci.* **32,** 799–805 (2012).

83. Vugt, B. van, Dagnino, B., Vartak, D., Safaai, H., Panzeri, S., Dehaene, S. & Roelfsema, P. R. The threshold for conscious report: Signal loss and response bias in visual and frontal cortex. *Science* **360,** 537–542 (2018).

84. Dehaene, S. & Changeux, J.-P. Experimental and theoretical approaches to conscious processing. *Neuron* **70,** 200–227 (2011).

85. Leech, R. & Sharp, D. J. The role of the posterior cingulate cortex in cognition and

disease. *Brain* **137,** 12–32 (2014).

86. Schubert, R., Ritter, P., Wüstenberg, T., Preuschhof, C., Curio, G., Sommer, W. & Villringer, A. Spatial Attention Related SEP Amplitude Modulations Covary with BOLD Signal in S1—A Simultaneous EEG—fMRI Study. *Cereb. Cortex* **18,** 2686–2700 (2008).

87. Dehaene, S. & Changeux, J.-P. Ongoing spontaneous activity controls access to consciousness: a neuronal model for inattentional blindness. *PLoS Biol.* **3,** e141 (2005).

88. Wang, X., Wu, Q., Egan, L., Gu, X., Liu, P., Gu, H., Yang, Y., Luo, J., Wu, Y., Gao, Z. & Fan, J. Anterior insular cortex plays a critical role in interoceptive attention. *Elife* **8,** (2019).

89. Jones, S. R., Kerr, C. E., Wan, Q., Pritchett, D. L., Hämäläinen, M. & Moore, C. I. Cued Spatial Attention Drives Functionally-Relevant Modulation of The Mu Rhythm in Primary Somatosensory Cortex. *J. Neurosci.* **30,** 13760 (2010).

90. Craddock, M., Poliakoff, E., El-deredy, W., Klepousniotou, E. & Lloyd, D. M. Pre-stimulus alpha oscillations over somatosensory cortex predict tactile misperceptions. *Neuropsychologia* **96,** 9–18 (2017).

91. Pang, J., Tang, X., Li, H., Hu, Q., Cui, H., Zhang, L., Li, W., Zhu, Z., Wang, J. & Li, C. Altered Interoceptive Processing in Generalized Anxiety Disorder—A Heartbeat-Evoked Potential Research. *Front. Psychiatry* **10,** 616 (2019).

92. Paulus, M. P. & Stein, M. B. Interoception in anxiety and depression. *Brain Struct. Funct.* **214,** 451–463 (2010).

93. Chen, Z., Venkat, P., Seyfried, D., Chopp, M., Yan, T. & Chen, J. Brain-Heart Interaction: Cardiac Complications after Stroke. *Circ. Res.* **121,** 451–468 (2017).

94. Stern, E. R., Grimaldi, S. J., Muratore, A., Murrough, J., Leibu, E., Fleysher, L., Goodman, W. K. & Burdick, K. E. Neural correlates of interoception: Effects of interoceptive focus and relationship to dimensional measures of body awareness. *Hum. Brain Mapp.* **38,** 6068–6082 (2017).

2 Statutory Declaration

I, *Esra Al*, by personally signing this document in lieu of an oath, hereby affirm that I prepared the submitted dissertation on the topic *The impact of heart-brain interactions on somatosensory perception* (*Der Einfluss von Herz-Hirn Interaktionen auf die somatosensorische Wahrnehmung)*, independently and without the support of third parties, and that I used no other sources and aids than those stated.

All parts which are based on the publications or presentations of other authors, either in letter or in spirit, are specified as such in accordance with the citing guidelines. The sections on methodology (in particular regarding practical work, laboratory regulations, statistical processing) and results (in particular regarding figures, charts and tables) are exclusively my responsibility.

Furthermore, I declare that I have correctly marked all of the data, the analyses, and the conclusions generated from data obtained in collaboration with other persons, and that I have correctly marked my own contribution and the contributions of other persons (cf. declaration of contribution). I have correctly marked all texts or parts of texts that were generated in collaboration with other persons.

My contributions to any publications to this dissertation correspond to those stated in the below joint declaration made together with the supervisor. All publications created within the scope of the dissertation comply with the guidelines of the ICMJE (International Committee of Medical Journal Editors; www.icmje.org) on authorship. In addition, I declare that I shall comply with the regulations of Charité – Universitätsmedizin Berlin on ensuring good scientific practice.

I declare that I have not yet submitted this dissertation in identical or similar form to another Faculty.

The significance of this statutory declaration and the consequences of a false statutory declaration under criminal law (Sections 156, 161 of the German Criminal Code) are known to me.

Date___24.03.2021_____   Signature_____

3 Declaration of Contribution to the Publications

Esra Al contributed the following to the below listed publication:

Al, E., Iliopoulos, F., Forschack, N., Nierhaus, T., Grund, M., Motyka, P., Gaebler, M., Nikulin, V. V. & Villringer, A. Heart-brain interactions shape somatosensory perception and evoked potentials. *Proc. Natl. Acad. Sci. U. S. A.* **117,** 10575–10584 (2020).

Impact Factor (2018) = 9.580

Contribution in detail:

- Esra Al developed the hypotheses as well as the experimental design of the present study in collaboration with the co-authors.
- She planned the practical implementation of the experiment and helped with the programming of the experiment scripts using PsychToolbox together with another coauthor, Fivos Iliopoulos.
- She ran the most of the experiments independently in the EEG laboratories of the Max Planck Institute for Human Cognitive and Brain Sciences. (In 25% of the experiments, another coauthor assisted the measurements).
- After consulting the co-authors, she assessed the quality of the EEG, ECG, and structural MRI data, preprocessed them using EEGLAB (based on Matlab), Kubios, and Freesurfer independently.
- Furthermore, she independently preprocessed EEG and ECG data using EEGLAB, custom-written scripts that she coded on Matlab and Rstudio. For example, she wrote scripts for the automatic categorization of cardiac phases for every trial of individual subjects in Rstudio. To clean the cardiac field and pulse artifacts from the EEG data thoroughly, she developed techniques and implemented them by writing Matlab scripts.
- She ran the source-level analysis on the EEG and structural MRI data by using Brainstorm (based on Matlab) and custom-written scripts.
- She performed statistical analysis using FieldTrip (based on Matlab), custom-written scripts on Rstudio, and Matlab.
- She independently carried out the graphic representation of the methods and results (i.e. the conceptualization and creation of all figures and tables for the publication) with feedback from the co-authors.

- For facilitating open science, she was responsible to upload all experimental scripts and data on Open Science Framework as well as the preprint on bioRxiv.
- As the first author of the publication, she carried out extensive literature research, interpreted the results, and wrote the drafts of the manuscript, which was then revised by the co-authors. She was responsible for coordinating the journal submission process and writing the responses to reviewers, which was then revised by her two supervisors.

Signature, date and stamp of the supervising
university teacher

Signature of the doctoral candidate

_____

_____

4 Extract from the Journal Summary List (ISI Web of KnowledgeSM)

Journal Data Filtered By: **Selected JCR Year: 2018** Selected Editions: SCIE,SSCI
Selected Categories: **"MULTIDISCIPLINARY SCIENCES"** Selected Category
Scheme: WoS
Gesamtanzahl: 69 Journale

Rank	Full Journal Title	Total Cites	Journal Impact Factor	Eigenfactor Score
1	NATURE	745,692	43.070	1.285010
2	SCIENCE	680,994	41.037	1.070190
3	National Science Review	1,842	13.222	0.006500
4	Science Advances	21,901	12.804	0.110010
5	Nature Communications	243,793	11.878	1.103290
6	Nature Human Behaviour	1,230	10.575	0.006550
7	PROCEEDINGS OF THE NATIONAL ACADEMY OF SCIENCES OF THE UNITED STATES OF AMERICA	661,118	9.580	1.022190
8	Science Bulletin	3,569	6.277	0.009840
9	Scientific Data	3,240	5.929	0.015610
10	Frontiers in Bioengineering and Biotechnology	1,994	5.122	0.006540
11	Journal of Advanced Research	2,691	5.045	0.004780
12	Research Synthesis Methods	1,932	5.043	0.005420
13	GigaScience	2,674	4.688	0.012510
14	Annals of the New York Academy of Sciences	46,385	4.295	0.025840
15	Scientific Reports	302,086	4.011	1.061540
16	Journal of the Royal Society Interface	12,933	3.224	0.029190
17	NPJ Microgravity	203	3.111	0.000670
18	PHILOSOPHICAL TRANSACTIONS OF THE ROYAL SOCIETY A-MATHEMATICAL PHYSICAL AND ENGINEERING SCIENCES	19,227	3.093	0.028200

Selected JCR Year: 2018; Selected Categories: "MULTIDISCIPLINARY SCIENCES"

5 Print Version of the Publication

Al, E., Iliopoulos, F., Forschack, N., Nierhaus, T., Grund, M., Motyka, P., Gaebler, M., Nikulin, V. V. & Villringer, A. Heart-brain interactions shape somatosensory perception and evoked potentials. *Proc. Natl. Acad. Sci. U. S. A.* **117,** 10575–10584 (2020).

Heart–brain interactions shape somatosensory perception and evoked potentials

Esra Al[a,b,c,1], Fivos Iliopoulos[a,c,d], Norman Forschack[a,e], Till Nierhaus[a,f], Martin Grund[a], Paweł Motyka[g], Michael Gaebler[a,b], Vadim V. Nikulin[a,h], and Arno Villringer[a,b,c,1]

[a]Department of Neurology, Max Planck Institute for Human Cognitive and Brain Sciences, 04103 Leipzig, Germany; [b]MindBrainBody Institute, Berlin School of Mind and Brain, Humboldt-Universität zu Berlin, 10099 Berlin, Germany; [c]Center for Stroke Research Berlin (CSB), Charité – Universitätsmedizin Berlin, 10117 Berlin, Germany; [d]International Max Planck Research School on the Life Course, Max Planck Institute for Human Development, 14195 Berlin, Germany; [e]Experimental Psychology and Methods, Faculty of Life Sciences, University of Leipzig, 04109 Leipzig, Germany; [f]Neurocomputation and Neuroimaging Unit, Department of Education and Psychology, Freie Universität Berlin, 14195 Berlin, Germany; [g]Faculty of Psychology, University of Warsaw, 00-927 Warsaw, Poland; and [h]Institute of Cognitive Neuroscience, National Research University Higher School of Economics, 101000 Moscow, Russia

Even though humans are mostly not aware of their heartbeats, several heartbeat-related effects have been reported to influence conscious perception. It is not clear whether these effects are distinct or related phenomena, or whether they are early sensory effects or late decisional processes. Combining electroencephalography and electrocardiography, along with signal detection theory analyses, we identify two distinct heartbeat-related influences on conscious perception differentially related to early vs. late somatosensory processing. First, an effect on early sensory processing was found for the heartbeat-evoked potential (HEP), a marker of cardiac interoception. The amplitude of the prestimulus HEP negatively correlated with localization and detection of somatosensory stimuli, reflecting a more conservative detection bias (criterion). Importantly, higher HEP amplitudes were followed by decreases in early (P50) as well as late (N140, P300) somatosensory-evoked potential (SEP) amplitudes. Second, stimulus timing along the cardiac cycle also affected perception. During systole, stimuli were detected and correctly localized less frequently, relating to a shift in perceptual sensitivity. This perceptual attenuation was accompanied by the suppression of only late SEP components (P300) and was stronger for individuals with a more stable heart rate. Both heart-related effects were independent of alpha oscillations' influence on somatosensory processing. We explain cardiac cycle timing effects in a predictive coding account and suggest that HEP-related effects might reflect spontaneous shifts between interoception and exteroception or modulations of general attentional resources. Thus, our results provide a general conceptual framework to explain how internal signals can be integrated into our conscious perception of the world.

consciousness | somatosensory awareness | body–brain interaction | EEG | rhythms

The neural response to an external stimulus and its access to consciousness depend on stimulus features as well as the state of the brain (1–5). Interestingly, functional states of other bodily organs, such as the heart, can also influence the perception of external stimuli. For example, several studies have reported that timing along the cardiac cycle (e.g., systole vs. diastole) impacts the perception of visual or auditory stimuli (refs. 6 and 7, but also see refs. 8 and 9 for nonsignificant heart phase-dependent effects). For the somatosensory system, we recently showed increased detection during diastole (10) similar to the other sensory domains (6, 7). Interestingly, a previous study had reported lower somatosensory sensibility during diastole (11) when stimulus presentation was at fixed time points during the cardiac cycle. Similar to perception, neural responses to visual and auditory stimuli are modulated across the cardiac cycle (12, 13). Most often they have been reported to be higher during diastole than systole (12, 13). A recent study (14) has also associated fluctuations of the heartbeat-evoked potential (HEP; refs. 15–17) with conscious detection of a visual stimulus.

While thus increasing evidence indicates that events related to cardiac function may modulate conscious perception, fundamental questions remain unanswered. Is it perceptual discrimination ability, that is, sensitivity in signal detection theory (SDT; ref. 18), that is influenced by cardiac activity? Or, might a bias to report the presence or absence of a stimulus underlie the effect, that is, criterion, in SDT? Are criterion-free decisions also affected by the heart? How are these perceptual effects reflected in evoked neural activity? More specifically, do these effects influence early, preconscious, somatosensory-evoked potentials (SEPs) or only the late components? Ultimately, how cardiac-related modulation of perceptual awareness relates to primary determinants of sensory perception and evoked brain activity, such as prediction, attention, and background neural activity, is unknown.

The current study targets mechanisms linking heart, brain, and perception using a somatosensory detection and localization task with electroencephalography (EEG) recordings. In an SDT-based design, we identify differential effects of two heartbeat-related phenomena: 1) stimulus timing during the cardiac cycle

> ## Significance
>
> Our brain continuously receives signals from the body and the environment. Although we are mostly unaware of internal bodily processes, such as our heartbeats, they can affect our perception. Here, we show two distinct ways in which the heartbeat modulates conscious perception. First, increased heartbeat-evoked neural activity before stimulation is followed by decreased somatosensory detection. This effect can be explained by subjects adopting a more conservative decision criterion, which is accompanied by changes in early and late somatosensory-evoked responses. Second, stimulus timing during the cardiac cycle affects sensitivity but not criterion for somatosensory stimuli, which is reflected only in late somatosensory-evoked responses. We propose that these heartbeat-related modulations are connected to fluctuations of interoceptive attention and (unconscious) predictive coding mechanisms.

NEUROSCIENCE

and 2) the amplitude of the HEP on somatosensory perception and evoked potentials. We argue that these findings are in line with a predictive coding account for cardiac phase-related sensory fluctuations and likely to be related to spontaneous shifts between interoception and exteroception as indexed by the HEP amplitude.

Results

Thirty-seven participants were presented weak somatosensory (electrical) stimuli to either the left index or middle finger in a combined yes/no detection and location discrimination task (Fig. 1). Both EEG and electrocardiography (ECG) were recorded. On average, participants detected $51.0 \pm 10.5\%$ (mean $\pm$ SD) of the somatosensory stimuli with a false alarm rate of $8.4 \pm 7.7\%$. This corresponds to a mean detection sensitivity, d', of 1.57 ± 0.57 and a decision criterion, c, of 0.76 ± 0.32. Participants correctly localized $73.3 \pm 6.6\%$ of stimuli (fingerwise), corresponding to a mean localization sensitivity of 0.90 ± 0.32. Participants correctly localized $88.9 \pm 7.9\%$ of hits and $57.0 \pm 6.9\%$ of misses.

Detection Varies across the Cardiac Cycle. We hypothesized that hits were more likely to occur in a later phase of the cardiac cycle, whereas misses would occur in an earlier phase (10). We used three complementary approaches to test this hypothesis. First, we used circular statistics (19), which allows an assessment of the entire cardiac cycle, without distinguishing systole and diastole, whose relative lengths are differentially affected by changes in the duration of the cardiac cycle (see *Circular Analysis* for details). A Rayleigh test showed that hits were not uniformly distributed, $\overline{R} = 0.40$, $P = 0.003$ (Fig. 2*A*), with a mean angle of $308.70°$ corresponding to the later cardiac cycle phase (i.e., diastole). Similarly, the distribution of misses was not uniform, $\overline{R} = 0.40$, $P = 0.004$ (Fig. 2*A*), with a mean angle of $93.84°$, located in the early phase of the cardiac cycle (i.e., systole). We observed a trend in the distribution of correct localizations toward the later phases of the cardiac cycle ($\overline{R} = 0.28$, $P = 0.067$). The distribution of wrong localizations was not significantly different from a uniform distribution, $\overline{R} = 0.17$, $P = 0.35$ (Fig. 2*A*).

Detection Rate and Sensitivity Are Higher during Diastole Compared to Systole. To account for the biphasic nature of the cardiac cycle, we also examined detection and localization performance by segmenting each cardiac cycle into systole and diastole: We operationalized the systolic time window for each cardiac cycle as the time between the R-peak and the end of the t-wave (see *Binary Analysis* for further details). Based on the duration of this
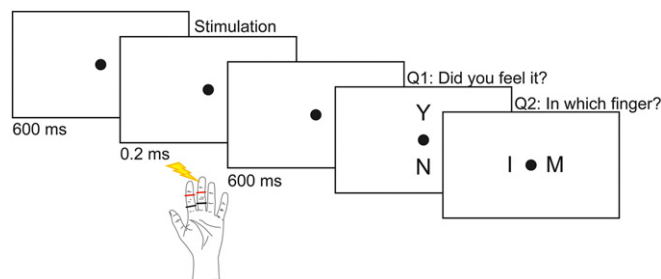

Fig. 1. Experimental paradigm. Thirty-seven subjects received a weak electrical pulse to the left index or the middle finger in 800 out of 960 trials over eight experimental blocks. Subjects were told that every trial contained a stimulus; however, in 160 pseudorandomized trials no stimulus was actually presented. In every trial, participants were asked to first perform a yes/no detection task and then a location discrimination task.

systolic window, we defined a diastolic window of equal length at the end of each cardiac cycle (Fig. 2*B*). As suggested by our first analysis, the detection rate for the weak stimuli was significantly higher during diastole (mean [M] = 52.41%) than systole (M = 49.53%), $t_{36} = -3.95$, $P = 3 \cdot 10^{-4}$ (Fig. 2*B*). Increased detection rate during diastole was observed for 27 out of 37 participants. However, the false alarm rate did not differ significantly between systole (M = 8.50%) and diastole (M = 8.19%), $t_{36} = 0.54$, $P = 0.59$. There was no significant difference between stimulus intensities in systole and diastole ($t_{36} = 0.57$, $P = 0.57$; *SI Appendix*, Table S1). Additionally, we tested whether the latency to response differed between systole and diastole but did not find a significant difference ($t_{36} = 0.83$, $P = 0.41$). We furthermore tested whether the effect of cardiac phase on detection correlated with the heart rate or the heart rate variability (HRV, i.e., the SD of time duration between two successive R-peaks [RR intervals]) of individuals. While there was no significant correlation between subject's heart rate and their detection rate variation between systole and diastole (Pearson's correlation, $r = 0.01$, $P = 0.95$), subjects' HRV negatively correlated with their detection rate difference ($r = -0.36$, $P = 0.03$; *SI Appendix*, Fig. S1).

SDT was applied to test whether the increased detection rates in diastole were due to increased perceptual sensitivity (d') or due to adopting a more liberal response strategy (criterion). Detection sensitivity was significantly higher in diastole (M = 1.59) than systole (M = 1.48), $t_{36} = -2.38$, $P = 0.008$ (Fig. 2*B*). For the criterion, no significant difference between systole (M = 0.75) and diastole (M = 0.73) was found, $t_{36} = 0.71$, $P = 0.48$. Localization performance was also tested across the cardiac cycle. Correct localization rate did not differ significantly between systole (M = 73.27%) and diastole (M = 73.68%), $t_{36} = -0.62$, $P = 0.54$. Likewise, localization sensitivity was not significantly different between systole (M = 0.90) and diastole (M = 0.93), $t_{36} = -0.89$, $P = 0.38$ (Fig. 2*B*).

Finally, other heartbeat-associated physiological events (e.g., the pulse wave) are temporally coupled with the onset of systole. Therefore, in an exploratory analysis we assessed the effect of the absolute time delay of somatosensory stimulation from the previous R-peak on detection and localization rates. Detection and localization rates were significantly different between four time windows: 0 to 200, 200 to 400, 400 to 600, and 600 to 800 ms (within-subject ANOVA, $F_{3,108} = 7.25$, $P = 2 \cdot 10^{-4}$ and $F_{3,108} = 3.97$, $P = 0.01$). Detection and localization was lowest 200 to 400 ms after the R-peak (post hoc paired t test between 0- to 200- and 200- to 400-ms windows for detection: $t_{36} = 3.76$, $P = 6 \cdot 10^{-4}$ and localization: $t_{36} = 2.88$, $P = 0.007$; between 200 to 400 and 400 to 600 ms for detection: $t_{36} = -3.61$, $P = 9 \cdot 10^{-4}$ and localization: $t_{36} = -1.36$, $P = 0.18$; Fig. 2*C*). Significant differences were found for the sensitivity (main effect of time, $F_{3,108} = 6.26$, $P = 6 \cdot 10^{-4}$; post hoc paired t test between 0 to 200 and 200 to 400 ms, $t_{36} = 2.83$, $P = 0.008$ and between 200 to 400 and 400 to 600 ms, $t_{36} = -3.48$, $P = 0.001$) but not for the criterion ($F_{3,108} = 0.10$, $P = 0.96$; *SI Appendix*, Fig. S2).

SEPs during Diastole Compared to Systole. Conscious somatosensory perception is known to correlate with greater amplitude of certain SEP components such as N140 and P300 (20). In line with the changes in somatosensory perception, we expected to find differences in SEPs during diastole compared to systole. We systematically compared SEPs during systole and diastole in the time window of 0 (stimulation onset) to 600 ms with a cluster-based permutation t test. SEPs over the contralateral somatosensory cortex (indexed by C4 electrode) showed greater positivity when stimulation was performed during diastole than systole in two temporal clusters: 268 to 340 ms and 392 to 468 ms (Monte Carlo $P = 0.004$ and $P = 0.003$, respectively, corrected for multiple comparisons in time; Fig. 3*A*). SEPs for hits during
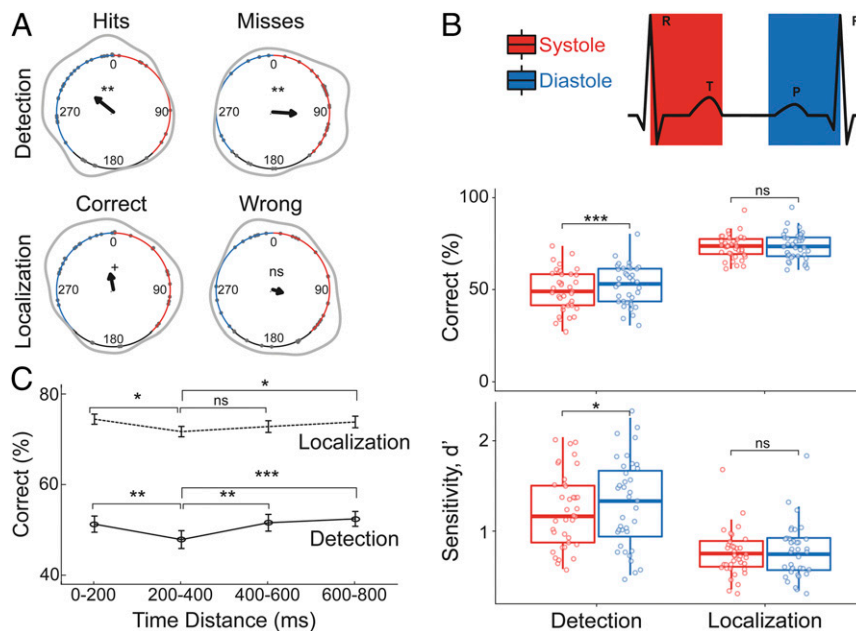
Fig. 2. Conscious detection of somatosensory stimuli varies across the cardiac cycle. (A) Distribution of hits (*Top Left*), misses (*Top Right*), correct localizations (*Bottom Left*), and wrong localizations (*Bottom Right*) across the cardiac cycle (the interval between two R-peaks at 0/360°). Gray points show subjects' mean degrees. The black arrows point toward the overall mean degree and its length indicates the coherence of individual means. The gray lines depict the circular density of individual means. The overall mean systole and diastole lengths are shown with red and blue, respectively. Hits and misses were nonuniformly distributed across the cardiac cycle (Rayleigh tests, $\overline{R} = 0.40$, $P = 0.003$ and $\overline{R} = 0.40$, $P = 0.004$, respectively). While correct localizations showed a trend toward a nonuniform distribution ($P = 0.067$), wrong localizations did not show a significant deviation from uniform distribution ($P = 0.35$). (B, *Top*) Correct detection and localization percentages during systole and diastole. Participants had more correct detections in diastole ($t_{36} = -3.95$, $P = 3 \cdot 10^{-4}$). No statistically significant difference between systole and diastole was found for correct localization ($P = 0.54$). (B, *Bottom*) Detection and localization sensitivity (d') between systole and diastole. Detection sensitivity was significantly higher in diastole than systole ($t_{36} = -2.38$, $P = 0.008$), and localization sensitivity did not differ significantly between the two cardiac phases ($P = 0.38$). (C) Correct detection and localization of somatosensory stimuli relative to their distance from the previous R-peak. Both detection and localization performances were lowest 200 to 400 ms after the R-peak. (post hoc paired t test between 0 and 200 and 200 and 400 ms for detection: $t_{36} = 3.76$, $P = 6 \cdot 10^{-4}$ and localization: $t_{36} = 2.88$, $P = 0.007$). Error bars represent SEMs. $^+P < 0.08$, $^*P < 0.05$, $^{**}P < 0.005$, $^{***}P < 0.0005$; ns, not significant.

diastole and systole did not differ significantly (smallest Monte Carlo $P = 0.27$). SEPs for misses, however, differed between systole and diastole over the contralateral somatosensory area. Higher positivity was observed in diastole compared to systole in time windows of 288 to 324 ms and 400 to 448 ms, respectively (Monte Carlo $P = 0.02$ and Monte Carlo $P = 0.01$, respectively; Fig. 3C).

We used a within-subject ANOVA with the factors detection (hit vs. miss) and cardiac phase (systole vs. diastole) to examine their effect on the P300 component of the SEPs. The P300 latency was determined in the 268- to 468-ms interval by merging the two time clusters observed for SEP differences between systole and diastole. We found significant main effects of detection ($F_{1,36} = 33.29$, $P = 1 \cdot 10^{-6}$) and cardiac phase ($F_{1,36} = 8.26$, $P = 0.007$). We did not observe a significant interaction effect ($F_{1,36} = 2.55$, $P = 0.12$).

To ascertain that the SEP differences during systole and diastole originate from somatosensory cortex, a source reconstruction was performed (see *SI Appendix, Methods* for details). On source level, we confirmed the significant difference in P300 amplitude during systole and diastole in the contralateral somatosensory cortex ($t_{36} = -2.55$, $P = 0.01$; *SI Appendix*, Fig. S3). In exploratory analyses, we tested SEPs in other brain areas known to influence heart–brain interactions and SEP amplitudes: right anterior insula (21), right inferior parietal lobule (rIPL; ref. 14), bilateral anterior and posterior cingulate (ACC and PCC; refs. 14 and 22) as well as bilateral lateral prefrontal cortices (LPFC; ref. 22). We did not find significant differences

in the SEPs between systole and diastole in these regions (*SI Appendix*, Table S2).

HEPs Predict Somatosensory Detection. HEPs are cortical electrophysiological responses time-locked to the R-peak of the ECG and are thought to represent neural processing of cardiac activity (15, 23, 24). We tested whether HEPs immediately preceding stimulus onset predicted somatosensory detection. To ensure that the time window for the HEP, 250 to 400 ms after the R-peak (15, 23, 24), was free of neural responses to the stimulation, we only included trials where the stimulus occurred at least 400 ms after the preceding R-peak (i.e., during diastole). We averaged the EEG data locked to the R-peak separately for hits and misses and submitted the 250- to 400-ms post R-peak time window to a cluster-based permutation t test. Prestimulus HEPs significantly differed between hits and misses over the contralateral somatosensory and central electrodes between 296 and 400 ms (Monte Carlo $P = 0.004$ corrected for multiple comparisons in space and time; Fig. 4 A and B) with a significantly higher positivity for misses. No significant changes were found in either heart rate or HRV between hits and misses included in the HEP analyses ($t_{36} = 1.51$, $P = 0.14$ and $t_{36} = -0.61$, $P = 0.55$, respectively). Therefore, the observed differences in HEPs cannot be attributed to changes in heart rate or HRV between hits and misses (14).

Subsequently, we calculated the prestimulus HEPs averaged across the cluster electrodes in the 296- to 400-ms time window separately for different detection responses (e.g., hits and misses). Similarly, we computed HEPs for cardiac cycles outside the
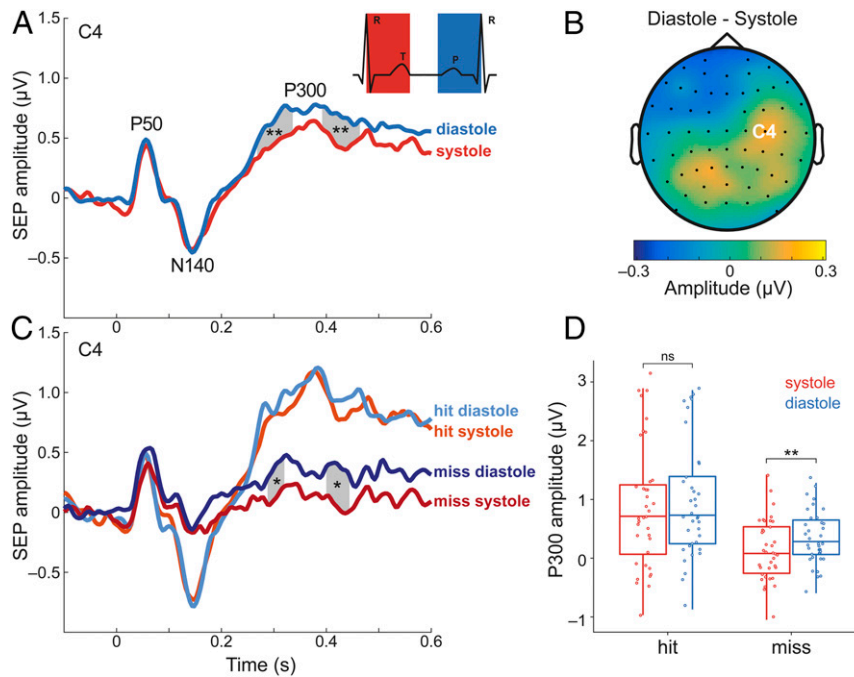
Fig. 3. SEPs for stimulations during systole vs. diastole (*A*) The difference in P300 component of SEPs (electrode C4) between systole and diastole. SEPs were more positive for stimuli during diastole than systole between 268 to 340 ms and 392 to 468 ms after stimulus onset over contralateral somatosensory cortex (Monte Carlo $P = 0.004$ and $P = 0.003$, respectively, corrected for multiple comparisons in time). (*B*) The topography contrast between diastole and systole between 268 and 468 ms. The position of electrode C4 is shown on the head model. (*C*) SEPs for hits (lighter colors) and misses (darker colors) during systole (red) and diastole (blue). SEPs showed higher positivity for misses during diastole than during systole in two time windows: 288 to 324 ms and 400 to 448 ms ($P = 0.02$ and $P = 0.01$, respectively). (*D*) The mean SEP amplitude between 268 to 468 ms for detection and cardiac phases. *$P < 0.05$, **$P < 0.005$; ns, not significant.

stimulation window (Fig. 1). Nonstimulation-related HEPs showed significantly more positivity than those preceding hits (paired t test, $t_{36} = 4.83$, $P = 3 \cdot 10^{-5}$) and a trend toward more positivity compared to those preceding misses (paired t test, $t_{36} = 1.90$, $P = 0.07$). HEP amplitudes preceding correct rejections showed significantly less positivity than HEPs preceding hits (paired t test, $t_{36} = 4.22$, $P = 2 \cdot 10^{-4}$) and were not significantly different from HEPs preceding misses (paired t test, $t_{36} = 1.63$, $P = 0.11$).

Next, we tested whether the HEP amplitude difference between hits and misses reflected a change in sensitivity or criterion according to SDT (Fig. 4 *D* and *E*). We sorted single trials according to mean HEP amplitude (across the cluster electrodes in the 296- to 400-ms time window) and split them into three equal bins (the number of HEP bins was chosen for comparability with a previous study; ref. 12) for each participant. We found that detection rates decreased as the HEP amplitude increased. Since we already showed this effect in the cluster statistics, we did not apply any statistical test here to avoid "double dipping" (25). The decrease in detection rate with increasing HEP amplitude was associated with an increase in criterion. More specifically, participants were more conservative in their decision and reported detecting the stimulus less often, regardless of their actual presence, when HEP amplitude was higher (within-subject ANOVA, $F_{2,36} = 10.30$, $P = 1 \cdot 10^{-4}$). Simultaneously, their sensitivity did not change significantly ($F_{2,72} = 0.17$, $P = 0.84$). We then tested whether prestimulus HEP amplitude could also affect somatosensory localization. Increasing HEP levels were associated with decreases in localization rate ($F_{1.72,62.01} = 10.27$, $P = 0.03$; Fig. 4*F*). Correct localization of hits and misses did not significantly differ between HEP bins ($F_{2,72} = 1.26$, $P = 0.29$ and $F_{2,72} = 0.28$, $P = 0.76$; *SI Appendix*, Fig. S4), indicating that the change in localization rate, associated with HEP amplitude, was connected with the change in detection rate.

We also tested whether prestimulus HEP amplitudes were associated with changes in SEP amplitudes. We applied a cluster-based permutation t test in the time window of 0 to 600 ms (0 = stimulation onset) to compare SEPs following low and high HEP amplitudes. Between 32 ms and 600 ms SEPs over the contralateral somatosensory cortex had higher positivity when stimulation was preceded by low HEP compared to high HEP amplitudes (Monte Carlo $P = 0.004$ corrected for multiple comparisons in time; Fig. 4*G*). On the source level, we confirmed that the amplitude of the earliest SEP component (P50) was significantly different following low and high HEP amplitudes in the contralateral primary somatosensory cortex (*SI Appendix*, Fig. S5). In further exploratory analyses, we tested whether differences in the P50 component could be observed in other brain areas involved in heart–brain interactions (cf. the previous section). Following high and low HEP amplitudes, there was a significant difference of P50 amplitude (false discovery rate-corrected) in the right anterior insula ($t_{36} = 3.23$, $P = 3 \cdot 10^{-3}$), the left and right PCC ($t_{36} = -4.55$, $P = 6 \cdot 10^{-5}$ and $t_{36} = -3.39$, $P = 2 \cdot 10^{-3}$), and the left and right LPFC ($t_{36} = -3.80$, $P = 5 \cdot 10^{-4}$ and $t_{36} = -4.14$, $P = 2 \cdot 10^{-4}$) but not in the rIPL and the bilateral ACC (*SI Appendix*, Table S3).

Prestimulus Sensorimotor Alpha Rhythm Predicts Somatosensory Detection and Localization. Given that alpha rhythm is known to influence sensory processing (2, 26–29), we assessed its effect on perception in our study as well as its possible interaction with heartbeat-related effects. Therefore, we sorted and divided trials into five equal bins (the number of alpha bins were chosen to be consistent with previous studies; refs. 25 and 26), according to the mean sensorimotor alpha amplitude between 300 and 0 ms before stimulus onset. We then calculated the percentage of correct detection and localization responses for every bin.
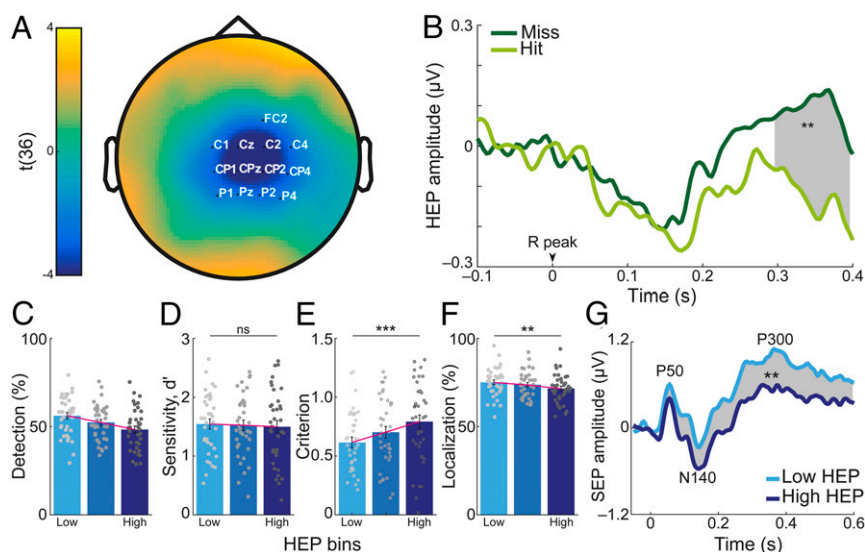
Fig. 4. HEPs before stimulus onset predicted somatosensory detection. (*A*) Topographical map of *t* values for HEP differences preceding hits and misses: Grand average across 37 participants in the 296- to 400-ms time window, where a significant difference (misses > hits) was observed on the highlighted electrodes (Monte Carlo $P = 0.004$ corrected for multiple comparisons in time and space). (*B*) Prestimulus HEPs averaged across the cluster. (*C–F*) Single-trials were sorted according to the mean HEP amplitude (across the cluster in the 296- to 400-ms time window) and split into three equal bins for each subject. (*C*) As the HEP amplitude increased, the detection rate decreased. (*D*) This decrease was not associated with a significant change in detection sensitivity ($P = 0.84$), (*E*) but correlated with an increase in criterion, that is, reporting stimulus presence less often regardless of actual stimulus presence ($P < 0.0005$). (*F*) Similar to the decrease in detection rate, correct localization rate decreased with increasing HEP amplitude ($P = 0.003$). The gray points on the bar plots represent individual subjects. (*G*) SEP amplitudes for trials in the low and high HEP bins. A significant difference in SEP amplitudes for the low and high HEP bin was observed between 32 and 600 ms poststimulation at contralateral somatosensory cortex (C4 electrode; Monte Carlo $P = 0.004$ corrected for multiple comparisons in time). Error bars represent SEMs. **$P < 0.005$, ***$P < 0.0005$; ns, not significant.

Correct detection and localization responses decreased with increasing levels of alpha amplitude (within-subject ANOVA, $F_{2.77,99.74} = 8.88$, $P = 3 \cdot 10^{-7}$ and $F_{3.30,118.81} = 6.11$, $P = 4 \cdot 10^{-5}$; Fig. 5*B*). With increasing prestimulus alpha amplitude, participants had a more conservative criterion ($F_{4,144} = 3.77$, $P = 0.006$; Fig. 5*C*). Sensitivity did not change significantly but showed a trend toward a decrease ($F_{4,14} = 2.20$, $P = 0.07$; Fig. 5*C*).

Sensorimotor Alpha Does Not Mediate Cardiac Phase Effect on Detection. Since prestimulus sensorimotor alpha amplitude modulated somatosensory perception, we hypothesized that alpha oscillations mediated the effect of cardiac phase on detection. To test this hypothesis, we calculated detection rates separately for systole and diastole trials within each alpha bin, where alpha amplitudes were comparable ($F_{1,36} = 0.89$, $P = 0.35$). Both cardiac phase and alpha levels significantly correlated with detection rate (within-subject ANOVA test, $F_{1,36} = 15.82$, $P = 3 \cdot 10^{-4}$ and $F_{2.93,105.30} = 12.05$, $P = 1 \cdot 10^{-6}$) but there was no significant interaction effect ($F_{4,144} = 0.34$, $P = 0.85$; Fig. 5*D*). This result indicated that detection rates differed between systole and diastole in the presence of comparable sensorimotor alpha amplitude levels. Further confirmation of this relationship by fitting general linear mixed-effects models (GLMM) at a single-trial level is shown in *SI Appendix, Methods* and Table S4).

Prestimulus Sensorimotor Alpha Does Not Mediate the Effect of HEP on Detection. To test whether prestimulus alpha amplitude mediated the relationship between HEP and detection, detection rates were calculated separately for low and high HEP levels within each alpha bin, where alpha amplitudes were similar between low and high HEP ($F_{1,36} = 0.14$, $P = 0.71$). A within-subject ANOVA showed significant main effects of both HEP ($F_{1,36} = 38.71$, $P = 4 \cdot 10^{-7}$) and alpha amplitude levels ($F_{4,144} = 10.37$, $P = 2 \cdot 10^{-7}$) for the detection rate with no significant interaction between them ($F_{4,144} = 0.75$, $P = 0.56$; Fig. 5*E*). This

result shows that the HEP effect was additive to the effect of alpha levels on detection (see also *SI Appendix*, Table S5 for additional GLMM analyses).

Controls for Volume Conduction Effect. Moreover, we ascertained that the observed SEP differences between the two cardiac phases as well as the HEP effect on detection were not likely to be explained by differences in cardiac electrical activity, which might have caused differences in the EEG by volume conduction (14, 16, 30). First, we examined whether possible ECG artifacts were successfully eliminated during the calculation of SEP differences between systole and diastole (see *Materials and Methods* for further details and *SI Appendix*, Fig. S6 *A–C*): We tested whether the ECG waveform difference between the systole and diastole trials were canceled out after ECG artifact correction (*SI Appendix*, Fig. S6 *D–F*). The comparison between two residual ECG waveforms for systole and diastole trials revealed no significant difference (no clusters were found; *SI Appendix*, Fig. S6F). Thus, the observed differences in SEP amplitudes between systole and diastole cannot be attributed to differences in cardiac electrical activity. Second, we checked whether the response to heartbeats preceding hits and misses differed in the ECG data. The ECG data looked similar for hits and misses (*SI Appendix*, Fig. S7A). The cluster statistics on the ECG data 296 to 400 ms after the R-peak did not show any significant difference between hits and misses (no clusters were found; *SI Appendix*, Fig. S7A). Correcting the EEG data for the cardiac artifact using independent component analysis did not significantly change the results (*SI Appendix*, Fig. S7B). Therefore, HEP differences preceding hits and misses cannot be explained due to differences in cardiac electrical activity.

Discussion

We show that the timing of a somatosensory stimulus, with respect to the cardiac cycle, along with the amplitude of the
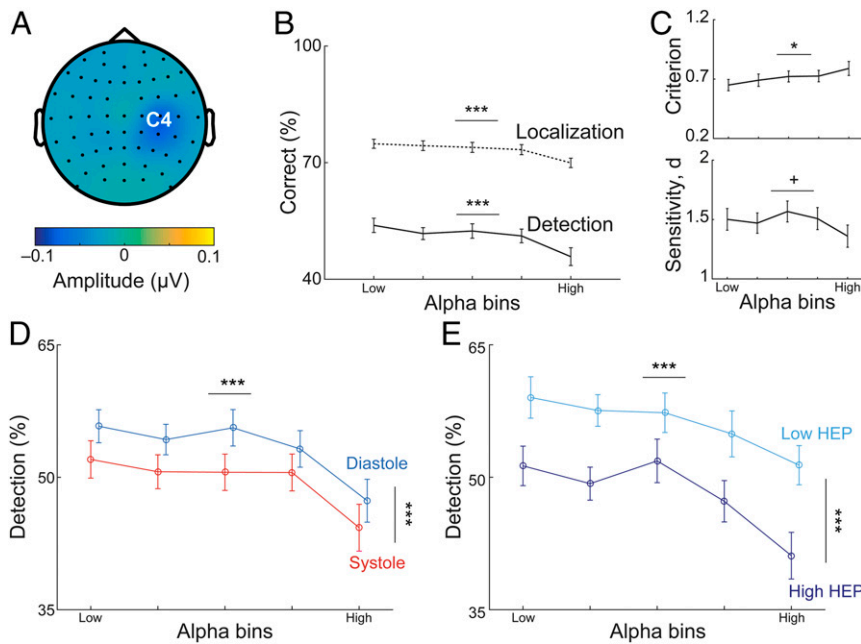
Fig. 5. Prestimulus sensorimotor alpha amplitude affects somatosensory perception but does not mediate heartbeat-related perceptual effects. (*A*) Topography of prestimulus alpha (8 to 13 Hz) difference between hits and misses in the time window of 300 to 0 ms before stimulus onset. (*B*) Trials were sorted into five equal bins of increasing mean sensorimotor alpha amplitudes in the prestimulus time window of 300 to 0 ms over contralateral somatosensory cortex (C4 electrode). Correct detection and localization rates are given for each alpha bin. Both detection and localization decreased as alpha amplitude levels increased ($P = 3 \cdot 10^{-7}$ and $P = 4 \cdot 10^{-5}$). (*C*) The decrease in detection rates with increasing alpha amplitude levels was associated with a significant increase in criterion, that is, a higher bias to miss the target ($P = 0.006$; *Top*) and a trend toward lower sensitivity ($P = 0.07$; *Bottom*). (*D*) For each alpha bin, detection rates are given separately for systole and diastole. Cardiac phase and alpha levels affected detection rate in an additive fashion (within-subject ANOVA test, $F_{1,36} = 15.82$, $P = 3 \cdot 10^{-4}$ and $F_{2.93,105.30} = 12.05$, $P = 1 \cdot 10^{-6}$). (*E*) For each alpha bin, detection rates are given separately for the trials with highest and lowest HEP, respectively. Prestimulus HEP amplitudes across the time window 296 to 400 ms after the R-peak were categorized in three equal bins for each participant, and detection rates were determined separately for the lowest and highest HEP conditions within each alpha bin. Both prestimulus factors, that is, HEP amplitudes and alpha amplitudes, influenced detection rates independently (within-subject ANOVA $F_{1,36} = 38.71$, $P = 4 \cdot 10^{-7}$ and $F_{4,144} = 10.37$, $P = 2 \cdot 10^{-7}$). Error bars represent SEMs. $^{+}P < 0.08$, $^{*}P < 0.05$, $^{***}P < 0.0005$.

prestimulus HEP shape conscious perception and the SEP. More specifically, detection rates were higher during diastole than systole and inversely related to the amplitude of the preceding HEP. Differential psychophysical effects of cardiac phase and HEP were observed on sensitivity and criterion, respectively. Furthermore, the cardiac phase influenced only late components of the SEPs (P300), whereas the effects of HEP amplitude were observed in both early (starting with P50) and late SEP components. While prestimulus alpha power also influenced perception and somatosensory processing, its effect was independent of both heartbeat-related effects on conscious perception, that is, alpha power and heartbeat-related events had an additive impact on somatosensory perception.

Our first main finding, the modulation of perception and neural response along the cardiac cycle, seems best explained by periodical modulations of perception in a predictive coding framework, in which the brain is continuously producing and updating a model of sensory input. This model not only concerns exteroceptive stimuli but also interoceptive signals such as the heartbeat. Each heartbeat and its concomitant pulse wave lead to transient physiological changes in the entire body. These repeating cardiac fluctuations are treated as predictable events and attenuated by the brain to minimize the likelihood of mistaking these self-generated signals as external stimuli (31, 32).

Of relevance for our study, heartbeat-related pressure fluctuations are tightly coupled with the firing pattern of afferent neurons in the fingers (33). These neurons fire in response to the pressure wave that reaches its maximum after around 200 to 400 ms after the R-peak within systole (34). We postulate that

the same top-down mechanism, which suppresses the perception of heartbeat-related firing changes in afferent finger neurons (33), also interferes with the perception of weak external stimuli to the fingers. This would only occur if presented during the same time period in systole—and more precisely between 200 and 400 ms after the R-peak. So, we propose that there is a prediction regarding heartbeat-/pulse wave-associated neural events which leads to the suppression of weak external somatosensory stimuli occurring in this time window. This effect reflected changes in sensitivity, that is, a weak input during systole is more likely to be regarded as pulse-associated "internal noise," and thus the differentiation between the stimulation and "noise" becomes more difficult. This could also explain why localization becomes worse during systole. Interestingly, a recent modeling study suggested that predictive mechanisms leading to attenuated integration of weak and neutral exteroceptive input might give rise to higher uncertainty about environmental "risks," which the organism would compensate for by increasing the expectation for detecting fear/threat in the environment (35). This may explain why the detection of fear/threat stimuli—in contrast to our neutral somatosensory stimuli—is enhanced during systole (36).

Furthermore, we show that perceptual suppression during systole was stronger in individuals who had less HRV. Whether this latter effect is related to a possibly more accurate (temporal) prediction of the next heartbeat or another physiological mechanism associated with HRV such as the vagal tone cannot be differentiated based on our data.

A reduction of the P300 amplitude accompanied the cardiac phase-associated modulation in somatosensory perception and sensitivity during systole compared to diastole. If a peripheral mechanism (e.g., less sensitivity of receptors of peripheral nerves) were to underlie the cardiac cycle effects on perception, it would yield already a difference in earlier SEP components. Interestingly, the P300 component has been regarded as an indicator of the "prediction error" (37) such that its amplitude is expected to reduce with a more precise prediction (via a smaller prediction error). Thus, the suppression of the P300 component during systole suggests that the pulse-synchronous peripheral neural activity (33) elicits a central prediction of this peripheral neural activity. The P300 component has been also suggested to be an indicator of conscious awareness (38, 39). Fittingly, the suppression of recurrent activity within the somatosensory network in the later stages of stimulus processing would be expected to reduce P300 amplitude (38–40). Taken together, the decreased P300 amplitude and lower sensitivity for somatosensory stimuli during systole might indicate a less efficient propagation of neuronal activity to higher processing levels (41). In the context of the global neural workspace theory (38), decreased sensitivity prevents "ignition" of conscious perception of a stimulus by interfering with its processing within the higher-order sensory cortices. This prevents the broadcasting of the stimulus and therefore conscious perception of it.

Our second main finding links HEP amplitudes to the processing of weak somatosensory stimuli. Specifically, we show that HEP in the time range of 296 to 400 ms showed higher positivity for misses than hits over centroparietal electrodes. That is, the amplitude (positivity) of HEP was inversely related to detection as well as stimulus localization. Although cardiac physiology is known to modulate HEP amplitudes (42, 43), we could not detect any changes in cardiovascular measures (heart rate and HRV) with respect to HEP. However, we cannot rule out a possible effect of cardiac physiology in HEP-related effects since we did not assess all cardiac-related measures such as cardiac output. In an SDT-based analysis, we have shown that the HEP effect was mainly related to changes in the criterion, in other words, with increasing HEP, participants adopted a more conservative bias for detection. A conservative bias has been shown to be associated with lower baseline firing rate across different brain regions, pushing neurons away from the threshold for "ignition" (41). Supporting this mechanism of criterion, that is, changing baseline firing rates in the brain, we found that the increasing prestimulus HEP amplitudes had a negative effect on the amplitude of both early (P50) and later SEP components (N140, P300). In other words, we interpret the changes in SEP amplitudes as reflecting changes in criterion.

Following different levels of HEP, the source-localized P50 amplitude was also different in contralateral somatosensory cortex, right insular cortex, LPFC, and PCC. Right anterior insula has been proposed as an integral hub to mediate internally and externally oriented attention (21) that can trigger attentional switches via its reciprocal connections with the lateral prefrontal cortex—an important region for attentional control similar to PCC (44). Similar modulation of early SEP components (P50) has previously been shown along with shifts of spatial attention (27, 45). Given that HEP amplitude has been found to be significantly higher during interoceptive compared to exteroceptive attention (46–48), we propose that the modulations of HEP amplitude reflect attentional shifts between external stimuli and internal bodily states. In line with this view, it has been suggested that the sudden "ignition" of a spontaneous internal activity can block external sensory processing (49). Similarly, heartbeat-related signals, which have been suggested to contribute to spontaneously active and self-directed states of consciousness (14), might prevent "ignition" of the upcoming somatosensory stimulus. Overall, the most plausible explanation for our findings

seems to be that a shift from external to internal attention, reflected by HEP amplitude increases, interferes with conscious perception of external somatosensory stimuli by decreasing the baseline firing rates within the somatosensory network. We are, however, aware that this interpretation is not definitely proven, and there might be alternative explanations, for example a modulation of overall attentional resources.

In the visual domain, a recent study also proposed that HEPs can predict the detection of weak stimuli (14). Interestingly, Park et al. (14) reported that larger heart-evoked activity measured using magnetoencephalography was associated with better external perception, while we observed the opposite pattern. These differences might be due to the different sensory modalities tested, that is, the allocation of attentional resources to interoception may vary for the detection of somatosensory and visual stimuli. In this context, it is important to note that interoception—in addition to neurotransmission via viscerosensory afferents—might be partly mediated or accompanied by somatic neurotransmission. For example, somatosensory afferents from the skin have been shown to be involved in cardiac interoception (50). Another interoceptive process, most likely to be informed by changes in the skin, is breathing. A recent study showed that when attention was directed to breathing, the somatosensory cortex showed a higher, and the visual cortex a lower, coupling to the anterior insular cortex, a key area for interoception (51). This result implies that interoception might interact with visual and somatosensory cortices differently. Furthermore, the somatosensory cortex has been indicated as one of the sources of HEPs (15, 52) and as playing a substantial role for interoception (21, 50). Therefore, it seems plausible that heart-related processes in the interoceptive cortices, notably involving somatosensory but less so visual areas, may interfere differently with the processing of exteroceptive somatosensory and visual signals.

Our third main finding relates heartbeat-associated effects to ongoing neural activity. First, we attempted to confirm the influence of prestimulus sensorimotor alpha activity on somatosensory perception as shown in previous studies (28, 53, 54). We observed that during periods of weak prestimulus alpha amplitude detection rates increased, which reflected a more liberal detection criterion. This finding is consistent with studies in the visual (26) and somatosensory domain (54). Even though detection has already been associated with lower alpha levels (2, 28, 53), the relationship between somatosensory localization and alpha amplitudes—to the best of our knowledge—has not been reported so far. In the visual domain, when localization and detection tasks were tested with a block design, detection but not localization was shown to vary across alpha levels (26). For the somatosensory domain, we showed that not only detection rates but also localization rates increased with decreasing prestimulus alpha amplitudes. Given the effect of alpha on somatosensory perception, we tested whether sensorimotor alpha oscillations modulated the heartbeat-related effects on detection. Our analysis showed that neither of the two heartbeat-related effects on perception (i.e., the cardiac phase and the HEP amplitude) was mediated by prestimulus alpha amplitude, but rather both are independent and additive to the effect of prestimulus sensorimotor alpha amplitude.

Several pathways relating cardiac activity to the brain have been suggested. Most notably, baroreceptor activation might inform cortical regions about timing and strength of each heartbeat (55). Baroreceptors are maximally activated during systole and their stimulation has been suggested to reduce cortical excitability (56). Thus, the systolic activation of baroreceptors might inform predictive mechanisms in the brain concerning when to attenuate the processing of heartbeat-coupled signals. Other than through baroreceptors, cardiac signals might also reach the cortex through direct projections of cardiac afferent neurons to the brain (57) or via somatosensory afferents on the

NEUROSCIENCE

skin (50) as discussed above. While presently it is not clear which of these pathways is most relevant for heart–brain interactions, our results are consistent with the notion of the somatosensory cortex as an important relay center for cardiac input (15, 21, 50, 52). How this relay center modulates the relationship between interoception and exteroception is an interesting topic for future research.

In conclusion, timing of stimulation along the cardiac cycle and spontaneous fluctuations of HEP amplitudes modulate access of weak somatosensory stimuli to consciousness and induce differential effects on SEPs. We explain these fundamental heart–brain interactions within the framework of interoceptive predictive coding (stimulus timing) and spontaneous shifts between interoception and exteroception (HEP amplitudes). These findings on heartbeat-related perceptual effects might serve as an example how in general body–brain interactions can shape our cognition.

Materials and Methods

Participants. Forty healthy volunteers were recruited from the database of the Max Planck Institute for Human Cognitive and Brain Sciences, Leipzig, Germany. Three subjects were excluded from the analysis due to technical problems during the experiment. Data from 37 subjects were analyzed (20 females, age: 25.7 ± 3.9 y [mean ± SD], range: 19 to 36 y). Some experimental blocks were excluded from the data analysis due to data acquisition failures (eight blocks from five subjects), false alarm rates >40% (eight blocks from eight subjects), responding with the wrong finger in the task (four blocks from three subjects), and observation of closed eyes during the task (three blocks from one subject). After these exclusions, a total of 274 experimental blocks with 32,880 trials in 37 subjects were analyzed. The study was approved by the Ethical Committee of the University of Leipzig's Medical Faculty (no. 462-15-01062015). All subjects signed written informed consent and were paid for their participation.

Somatosensory Stimulation and Task Design. Electrical finger nerve stimulation was performed with a constant-current stimulator (DS5; Digitimer) using single square-wave pulses with a duration of 200 μs. Steel wire ring electrodes were placed on the middle (anode) and the proximal (cathode) phalanx of the index and the middle finger of the left hand, respectively.

In the experiment, participants performed a yes/no detection and a two-alternative forced-choice localization task on every trial. At the beginning of each trial, a black dot appeared on the screen for 600 ms. Participants then expected to get stimulation on either the index or the middle finger of their left hand. Six hundred milliseconds after the stimulation, participants "were asked" (via "yes/no?" on the screen) to report as quickly as possible whether they felt a stimulus on one of their fingers or not. They responded "yes" if they felt the stimulus and "no" if not by using their right index finger. Thereafter, participants were asked to answer where the stimulation has occurred. They were explicitly told "to guess" even if they reported not feeling the stimulus in the first question. If they located the stimulus on the left index finger, they were asked to use their right index finger to answer and to use their right middle finger if they located the stimulus on the left middle finger. The next trial started immediately after responding to the localization question. In total, every participant completed eight blocks. Each block contained 100 trials with electrical stimulation (50 trials for each finger) and 20 trials without any stimulation (catch trials). The duration of each block was ~8 min. To find stimulus intensities with 50% detection probability (i.e., threshold), we applied a two-step procedure before starting the experiment. First, we roughly estimated the lowest stimulus intensity for which participants could report a sensation by applying the method of limits with ascending intensities separately for the index and the middle finger (27, 58). Second, we used a yes/no detection task (as described above) containing catch trials and six stimulus intensities around this predicted stimulus intensity (15% below, identical to, 20%, 40%, 60%, and 80% above) for each finger. The 50% threshold intensity for each finger was estimated from the participant's psychometric function (59). To control for threshold stability, stimulus intensities were readjusted after each block.

Hit, miss, false alarm (FA), and correct rejection (CR) terms were calculated for the yes/no detection task in this study. A hit was reporting the presence of a stimulus when it was present; a miss was reporting the absence of a stimulus even though it was present. For catch trials (i.e., no stimulus was presented), an FA was reporting the presence of a stimulus, while a CR was reporting its absence. The terms "correct localization" and "wrong localization" were

used to describe the localization task performance. Correct localization was reporting the stimulus location correctly; wrong localization was reporting it incorrectly.

Recordings. EEG was recorded from 62 scalp positions distributed over both hemispheres according to the international 10–10 system, using a commercial EEG acquisition system (actiCap, BrainAmp; Brain Products). The midfrontal electrode (FCz) was used as the reference and an electrode placed on the sternum as the ground. Electrode impedance was kept ≤5 kΩ for all channels. EEG was recorded with a bandpass filter between 0.015 Hz and 1 kHz and digitized with a sampling rate of 2.5 kHz. An ECG electrode connected to the EEG system was placed under the participant's left breast to record the heart activity.

Data Analysis. We applied two complementary approaches—circular and binary analysis—to examine detection and localization across the cardiac cycle (60). For these analyses, we first extracted the R-peaks from the ECG data by using Kubios HRV Analysis Software 2.2 (The Biomedical Signal and Medical Imaging Analysis Group, Department of Applied Physics, University of Kuopio, Finland) and visually corrected for inaccurately determined R-peaks (<0.1%). From RR interval time series during the whole experiment, we calculated the SD of RR intervals (SDNN) and natural-log transformed SDNN values to calculate HRV (61, 62).

Circular Analysis. We tested detection and localization over the entire cardiac cycle, from one R-peak to the next one, by using circular statistics, which corrects for different durations of the cardiac cycle both inter- and intra-individually and accounts for its oscillatory nature (19). We calculated the relative position of the stimulus onset within the cardiac cycle with the following formula:

$$[(\text{onset time–previous R-peak time})/(\text{subsequent R} - \text{peak time–previous R} - \text{peak time})] \times 360,$$

which resulted in values between 0° and 360° (0 indicating the R-peak before stimulus onset). The distribution of stimulus onsets was tested individually for each participant with a Rayleigh test for uniformity. Two participants were excluded from further circular analyses due to nonuniformly distributed stimulation onsets across the cardiac cycle ($\bar{R} = 0.06$, $P = 0.04$; $\bar{R} = 0.06$, $P = 0.03$). For the rest of the participants ($n = 35$), the assumption of uniform onset distributions was fulfilled. We calculated the mean phase value at which different performances occurred (detection task: hit and miss; localization task: correct localization and wrong localization) for each participant. At the group level, it was tested whether the distribution of a specific performance score (e.g., hits) deviated from the uniform distribution with Rayleigh tests (19). The Rayleigh test depends on the mean vector length out of a sample of circular data points and calculates the mean concentration of these phase values around the circle. A statistically significant Rayleigh test result indicates the nonuniform distribution of data around the circle, that is, the cardiac cycle.

Binary Analysis. Considering the biphasic nature of cardiac activity, detection and localization performances were compared between the systolic and diastolic phases of the cardiac cycle. We defined systole as the time between the R-peak and the end of the t-wave (10). We used the systolic length of each cardiac cycle to define diastole as a diastolic window of equal length placed at the end of the cardiac cycle. The equal length of systole and diastole was used to equate the probability of having a stimulus onset in the two phases of the cardiac cycle. To determine the end of t-wave, a trapezoidal area algorithm was applied in each trial (63). This method has advantages compared to an approach with fixed bins (e.g., defining systole as the 300-ms time window following the R-peak) because it accounts for within- and between-subject variations in the length of systole and diastole (i.e., the heart rate). The results of the automated algorithm were visually quality-controlled. Twenty-seven trials for which the algorithm failed to calculate t-wave end and produced an abnormal systole length (more than 4 SDs above or below the participant-specific mean systole) were removed from further binary analyses. Mean systole (and diastole) length obtained from these analyses was 333 ± 21 ms. Each trial was categorized depending on whether the stimulus occurred during systole or diastole. The average number of trials categorized as systole was 338 ± 51 and as diastole was 342 ± 59.

Data Preprocessing. EEG and ECG data were analyzed offline using EEGLAB (64) and FieldTrip (65) toolbox algorithms as well as custom-built scripts on a MATLAB platform (MathWorks Inc.). An antialiasing filter with a 112.5-Hz cutoff was used before down-sampling individual datasets to 250 Hz. After all blocks were concatenated, data were first high-pass-filtered with 0.5 Hz and then low-pass-filtered with 45 Hz using a fourth order of Butterworth filter. The EEG channels that had a flat line longer than 5 s or showed less than 85% correlation with its reconstructed activity from other channels were removed and interpolated using their neighboring channels. After a principal component analysis was applied, data underwent an independent component analysis (ICA) using an extended infomax algorithm to remove sources of heartbeat, ocular and muscle artifacts (66). ICA components with cardiac field artifact were determined by segmenting ICA components depending on the R-peak of the ECG electrode and visually selecting the components whose activities were matching the time course of R-peak and t-wave of the ECG. After removing artifactual ICA components, the artifact-free components were forward-projected for the subsequent analysis steps. Afterward, the data were rereferenced to the average reference.

SEP. Data were segmented from −1,000 to 2,000 ms with respect to stimulus onset separately for trials where the stimulation occurred during systole vs. diastole. After segmenting data, we performed baseline correction using 100- to 0-ms prestimulus window. Testing for the maximum positive deflection of the early SEP component P50 (40 to 60 ms) showed that the right primary somatosensory area, contralateral to the stimulated hand (67), was represented by the C4 electrode. Therefore, the statistical analysis of SEP amplitude was performed on the C4 electrode (68). To cancel out possible effects of blood circulation, we estimated the cardiac artifact in the EEG data. For this purpose, random triggers were placed over cardiac cycles outside the stimulation window (Fig. 1). Then, we classified the arbitrary triggers as systole or diastole depending on the position of the trigger in the cardiac cycle. After the classification, data were segmented around these triggers (−1,000 to 2,000 ms) and averaged separately for systole and diastole to estimate the cardiac artifact during systole and diastole for each EEG channel per subject. We baseline-corrected these signals 100 ms before the onset of the arbitrary triggers (*SI Appendix*, Fig. S7). To prevent any possible ECG-induced artifact on the SEPs, we subtracted the mean systolic and diastolic artifacts from the SEPs during systole and diastole trials, respectively (30).

HEPs. After preprocessing data as described above, we selected the cardiac cycles containing a stimulus. We only chose the trials in which the stimulus onset was at least 400 ms after the preceding R-peak (corresponding to diastole). We determined HEPs by segmenting the preprocessed EEG data from −1,000 to 2,000 ms around the R-peak separately for hits and misses as well as for correct localizations and wrong localizations. In this way, we could calculate the prestimulus HEPs, which have been reported between 250 and 400 ms after the R-peak (15, 23, 24).

Time-Frequency Analyses. We performed time-frequency analyses to investigate sensorimotor alpha activity locked to stimulus onset. For sensorimotor alpha, we selected ICA components representing sensorimotor rhythms to eliminate effects of the occipital alpha activity as described previously by our group (27, 68). One to seven components per participant (mean 3 ± 1 SD) were selected and included in the analysis of somatosensory oscillatory activity. We ensured that our selection of sensorimotor components corresponded to a source in primary somatosensory and motor areas in source level (see *SI Appendix*, Fig. S8 for details). Then, data were segmented (−1,000 to 2,000 ms) and ECG-induced artifacts for systole and

diastole were calculated and subtracted from the data as described in the previous section. Morlet wavelet analysis was performed on every trial for frequencies from 5 to 40 Hz with number of cycles increasing linearly from 4 to 10. Thus, a wavelet at 10 Hz was 4.9 cycles long and had a temporal resolution of 0.10 s and a spectral resolution of 4.85 Hz. We focused on the effects of prestimulus alpha activity in our statistical analysis to test whether the perceptual effect of the cardiac cycle on detection is influenced by prestimulus oscillatory activity (−300 to 0 ms) over contralateral somatosensory area.

Analyses according to SDT. Sensitivity (d') and criterion (c, response bias) were calculated according to SDT (69): d' and c were calculated as $z(HR) − z(FAR)$ and $−[z(HR) + z(FAR)]/2$, respectively, with HR corresponding to hit rate and FAR corresponding to false alarm rate. A log-linear correction was used to compensate for extreme false alarm proportions (70) since 2 of the 37 participants produced no false alarms. Localization d' prime was calculated as $\sqrt{2} * z$(correct localization rate).

Statistical Analyses. Assessment of statistical significance for "two-condition comparisons" in EEG data were based on cluster-based permutation t tests as implemented in the FieldTrip toolbox (65, 71). In this procedure, adjacent spatiotemporal or spatiospectrotemporal points for which t values exceed a threshold are clustered (cluster threshold P value: 0.05). Then the cluster statistics are calculated by taking the sum of t values of all points within each cluster. The type I error rate was controlled by evaluating the cluster-level statistics under a randomized null distribution of the maximum cluster-level statistics. To determine the distribution of maximal cluster-level statistics obtained by chance, condition labels were randomly shuffled 1,000 times. For each of these randomizations, cluster-level statistics were computed and the largest cluster-level statistic was entered into the null distribution. Finally, the experimentally observed cluster-level statistic was compared against the null distribution. Clusters with a P value below 0.05 (two-tailed) were considered "significant." We expected to observe differences in SEPs over contralateral somatosensory cortex indexed by C4 electrode. Therefore, in the comparisons of somatosensory related activity, we only used cluster statistics to test whether two experimental conditions differed in time over contralateral somatosensory cortex. In contrast, we did not a priori define a spatial region for HEP analyses but expected to observe a HEP between 250 and 400 ms after the R-peak (15, 23, 24).

If the sphericity assumption was violated in within-subject ANOVA, Greenhouse–Geisser correction was applied. All statistical tests were two-sided.

Data and Code Availability. The consent forms signed by participants do not allow us to give free access to data but require us to check that data are shared with members of the scientific community. Therefore, we stored data and code in the Open Science Framework and will make the link available upon request to researchers.

1. A. Arieli, A. Sterkin, A. Grinvald, A. Aertsen, Dynamics of ongoing activity: Explanation of the large variability in evoked cortical responses. *Science* **273**, 1868–1871 (1996).
2. H. van Dijk, J.-M. Schoffelen, R. Oostenveld, O. Jensen, Prestimulus oscillatory activity in the alpha band predicts visual discrimination ability. *J. Neurosci.* **28**, 1816–1823 (2008).
3. F. Blankenburg et al., Imperceptible stimuli and sensory processing impediment. *Science* **299**, 1864 (2003).
4. N. Weisz et al., Prestimulus oscillatory power and connectivity patterns predispose conscious somatosensory perception. *Proc. Natl. Acad. Sci. U.S.A.* **111**, E417–E425 (2014).
5. H. Gelbard-Sagiv, L. Mudrik, M. R. Hill, C. Koch, I. Fried, Human single neuron activity precedes emergence of conscious perception. *Nat. Commun.* **9**, 2057 (2018).
6. S. A. Saxon, Detection of near threshold signals during four phases of cardiac cycle. *Ala. J. Med. Sci.* **7**, 427–430 (1970).
7. C. A. Sandman, T. R. McCanne, D. N. Kaiser, B. Diamond, Heart rate and cardiac phase influences on visual perception. *J. Comp. Physiol. Psychol.* **91**, 189–202 (1977).
8. R. Elliott, V. Graf, Visual sensitivity as a function of phase of cardiac cycle. *Psychophysiology* **9**, 357–361 (1972).
9. L. F. Delfini, J. J. Campos, Signal detection and the "cardiac arousal cycle". *Psychophysiology* **9**, 484–491 (1972).
10. P. Motyka et al., Interactions between cardiac activity and conscious somatosensory perception. *Psychophysiology* **56**, e13424 (2019).
11. L. Edwards, C. Ring, D. McIntyre, J. B. Winer, U. Martin, Sensory detection thresholds are modulated across the cardiac cycle: Evidence that cutaneous sensibility is greatest for systolic stimulation. *Psychophysiology* **46**, 252–256 (2009).
12. B. B. Walker, C. A. Sandman, Visual evoked potentials change as heart rate and carotid pressure change. *Psychophysiology* **19**, 520–527 (1982).
13. C. A. Sandman, Augmentation of the auditory event related potentials of the brain during diastole. *Int. J. Psychophysiol.* **2**, 111–119 (1984).
14. H.-D. Park, S. Correia, A. Ducorps, C. Tallon-Baudry, Spontaneous fluctuations in neural responses to heartbeats predict visual detection. *Nat. Neurosci.* **17**, 612–618 (2014).

NEUROSCIENCE

15. M. Kern, A. Aertsen, A. Schulze-Bonhage, T. Ball, Heart cycle-related effects on event-related potentials, spectral power changes, and connectivity patterns in the human ECoG. *Neuroimage* **81**, 178–190 (2013).

16. P. Montoya, R. Schandry, A. Müller, Heartbeat evoked potentials (HEP): Topography and influence of cardiac awareness and focus of attention. *Electroencephalogr. Clin. Neurophysiol.* **88**, 163–172 (1993).

17. O. Pollatos, R. Schandry, Accuracy of heartbeat perception is reflected in the amplitude of the heartbeat-evoked brain potential. *Psychophysiology* **41**, 476–482 (2004).

18. D. M. Green, J. A. Swets, *Signal Detection Theory and Psychophysics* (Wiley, 1966).

19. A. Pewsey, M. Neuhäuser, G. Ruxton, *Circular Statistics in R* (Oxford University Press, 2013).

20. R. Auksztulewicz, F. Blankenburg, Subjective rating of weak tactile stimuli is parametrically encoded in event-related potentials. *J. Neurosci.* **33**, 11878–11887 (2013).

21. H. D. Critchley, S. Wiens, P. Rotshtein, A. Öhman, R. J. Dolan, Neural systems supporting interoceptive awareness. *Nat. Neurosci.* **7**, 189–195 (2004).

22. J. Hirvonen, S. Palva, Cortical localization of phase and amplitude dynamics predicting access to somatosensory awareness. *Hum. Brain Mapp.* **37**, 311–326 (2016).

23. R. Schandry, B. Sparrer, R. Weitkunat, From the heart to the brain: A study of heartbeat contingent scalp potentials. *Int. J. Neurosci.* **30**, 261–275 (1986).

24. R. Schandry, R. Weitkunat, Enhancement of heartbeat-related brain potentials through cardiac awareness training. *Int. J. Neurosci.* **53**, 243–253 (1990).

25. N. Kriegeskorte, W. K. Simmons, P. S. F. Bellgowan, C. I. Baker, Circular analysis in systems neuroscience: The dangers of double dipping. *Nat. Neurosci.* **12**, 535–540 (2009).

26. L. Iemi, M. Chaumon, S. M. Crouzet, N. A. Busch, Spontaneous neural oscillations bias perception by modulating baseline excitability. *J. Neurosci.* **37**, 807–819 (2017).

27. N. Forschack, T. Nierhaus, M. M. Müller, A. Villringer, Alpha-band brain oscillations shape the processing of perceptible as well as imperceptible somatosensory stimuli during selective attention. *J. Neurosci.* **37**, 6983–6994 (2017).

28. R. Schubert, S. Haufe, F. Blankenburg, A. Villringer, G. Curio, Now you'll feel it, now you won't: EEG rhythms predict the effectiveness of perceptual masking. *J. Cogn. Neurosci.* **21**, 2407–2419 (2009).

29. S. Haegens, V. Nácher, R. Luna, R. Romo, O. Jensen, α-Oscillations in the monkey sensorimotor network influence discrimination performance by rhythmical inhibition of neuronal spiking. *Proc. Natl. Acad. Sci. U.S.A.* **108**, 19377–19382 (2011).

30. M. A. Gray, L. Minati, G. Paoletti, H. D. Critchley, Baroreceptor activation attenuates attentional effects on pain-evoked potentials. *Pain* **151**, 853–861 (2010).

31. L. F. Barrett, W. K. Simmons, Interoceptive predictions in the brain. *Nat. Rev. Neurosci.* **16**, 419–429 (2015).

32. A. K. Seth, K. J. Friston, Active interoceptive inference and the emotional brain. *Philos. Trans. R. Soc. B* **371**, 20160007 (2016).

33. V. G. Macefield, Cardiovascular and respiratory modulation of tactile afferents in the human finger pad. *Exp. Physiol.* **88**, 617–625 (2003).

34. M. H. N. van Velzen, A. J. Loeve, S. P. Niehof, E. G. Mik, Increasing accuracy of pulse transit time measurements by automated elimination of distorted photoplethysmography waves. *Med. Biol. Eng. Comput.* **55**, 1989–2000 (2017).

35. M. Allen, A. Levy, T. Parr, K. J. Friston, In the body's eye: The computational anatomy of interoceptive inference. bioRxiv:10.1101/603928 (10 April 2019).

36. S. N. Garfinkel et al., Fear from the heart: Sensitivity to fear stimuli depends on individual heartbeats. *J. Neurosci.* **34**, 6573–6582 (2014).

37. K. Friston, A theory of cortical responses. *Philos. Trans. R. Soc. B* **360**, 815–836 (2005).

38. S. Dehaene, C. Sergent, J.-P. Changeux, A neuronal network model linking subjective reports and objective physiological data during conscious perception. *Proc. Natl. Acad. Sci. U.S.A.* **100**, 8520–8525 (2003).

39. R. Auksztulewicz, B. Spitzer, F. Blankenburg, Recurrent neural processing and somatosensory awareness. *J. Neurosci.* **32**, 799–805 (2012).

40. V. A. F. Lamme, Towards a true neural stance on consciousness. *Trends Cogn. Sci. (Regul. Ed.)* **10**, 494–501 (2006).

41. B. van Vugt et al., The threshold for conscious report: Signal loss and response bias in visual and frontal cortex. *Science* **360**, 537–542 (2018).

42. R. Schandry, P. Montoya, Event-related brain potentials and the processing of cardiac activity. *Biol. Psychol.* **42**, 75–85 (1996).

43. M. A. Gray et al., A cortical potential reflecting cardiac function. *Proc. Natl. Acad. Sci. U.S.A.* **104**, 6818–6823 (2007).

44. R. Leech, D. J. Sharp, The role of the posterior cingulate cortex in cognition and disease. *Brain* **137**, 12–32 (2014).

45. R. Schubert et al., Spatial attention related SEP amplitude modulations covary with BOLD signal in S1-A simultaneous EEG–fMRI study. *Cereb. Cortex* **18**, 2686–2700 (2008).

46. M. Villena-González et al., Attending to the heart is associated with posterior alpha band increase and a reduction in sensitivity to concurrent visual stimuli. *Psychophysiology* **54**, 1483–1497 (2017).

47. I. García-Cordero et al., Attention, in and out: Scalp-level and intracranial EEG correlates of interoception and exteroception. *Front. Neurosci.* **11**, 411 (2017).

48. F. H. Petzschner et al., Focus of attention modulates the heartbeat evoked potential. *Neuroimage* **186**, 595–606 (2019).

49. S. Dehaene, J.-P. Changeux, Ongoing spontaneous activity controls access to consciousness: A neuronal model for inattentional blindness. *PLoS Biol.* **3**, e141 (2005).

50. S. S. Khalsa, D. Rudrauf, J. S. Feinstein, D. Tranel, The pathways of interoceptive awareness. *Nat. Neurosci.* **12**, 1494–1496 (2009).

51. X. Wang et al., Anterior insular cortex plays a critical role in interoceptive attention. *eLife* **8**, e42265 (2019).

52. O. Pollatos, W. Kirsch, R. Schandry, Brain structures involved in interoceptive awareness and cardioafferent signal processing: A dipole source localization study. *Hum. Brain Mapp.* **26**, 54–64 (2005).

53. S. R. Jones et al., Cued spatial attention drives functionally relevant modulation of the mu rhythm in primary somatosensory cortex. *J. Neurosci.* **30**, 13760–13765 (2010).

54. M. Craddock, E. Poliakoff, W. El-Deredy, E. Klepousniotou, D. M. Lloyd, Pre-stimulus alpha oscillations over somatosensory cortex predict tactile misperceptions. *Neuropsychologia* **96**, 9–18 (2017).

55. H. D. Critchley, S. N. Garfinkel, The influence of physiological signals on cognition. *Curr. Opin. Behav. Sci.* **19**, 13–18 (2018).

56. H. Rau, T. Elbert, Psychophysiology of arterial baroreceptors and the etiology of hypertension. *Biol. Psychol.* **57**, 179–201 (2001).

57. H.-D. Park, O. Blanke, Heartbeat-evoked cortical responses: Underlying mechanisms, functional roles, and methodological considerations. *Neuroimage* **197**, 502–511 (2019).

58. B. Taskin, S. Holtze, T. Krause, A. Villringer, Inhibitory impact of subliminal electrical finger stimulation on SI representation and perceptual sensitivity of an adjacent finger. *Neuroimage* **39**, 1307–1313 (2008).

59. W. H. Ehrenstein, A. Ehrenstein, *Psychophysical Methods* (Springer, 1999).

60. S. Kunzendorf et al., Active information sampling varies across the cardiac cycle. *Psychophysiology* **56**, e13322 (2019).

61. M. P. Tarvainen, J.-P. Niskanen, J. A. Lipponen, P. O. Ranta-Aho, P. A. Karjalainen, Kubios HRV–Heart rate variability analysis software. *Comput. Methods Programs Biomed.* **113**, 210–220 (2014).

62. F. Shaffer, J. P. Ginsberg, An overview of heart rate variability metrics and norms. *Front. Public Heal.* **5**, 258 (2017).

63. C. R. Vázquez-Seisdedos, J. E. Neto, E. J. Marañón Reyes, A. Klautau, R. C. Limão de Oliveira, New approach for T-wave end detection on electrocardiogram: Performance in noisy conditions. *Biomed. Eng. Online* **10**, 77 (2011).

64. A. Delorme, S. Makeig, EEGLAB: An open source toolbox for analysis of single-trial EEG dynamics including independent component analysis. *J. Neurosci. Methods* **134**, 9–21 (2004).

65. R. Oostenveld, P. Fries, E. Maris, J.-M. Schoffelen, FieldTrip: Open source software for advanced analysis of MEG, EEG, and invasive electrophysiological data. *Comput. Intell. Neurosci.* **2011**, 156869 (2011).

66. A. Delorme, J. Palmer, J. Onton, R. Oostenveld, S. Makeig, Independent EEG sources are dipolar. *PLoS One* **7**, e30135 (2012).

67. Y. Zhang, M. Ding, Detection of a weak somatosensory stimulus: Role of the prestimulus mu rhythm and its top-down modulation. *J. Cogn. Neurosci.* **22**, 307–322 (2010).

68. T. Nierhaus et al., Imperceptible somatosensory stimulation alters sensorimotor background rhythm and connectivity. *J. Neurosci.* **35**, 5917–5925 (2015).

69. N. Macmillan, C. Creelman, *Detection Theory: A User's Guide* (Psychology Press, 2004).

70. M. J. Hautus, Corrections for extreme proportions and their biasing effects on estimated values of d'. *Behav. Res. Methods Instrum. Comput.* **27**, 46–51 (1995).

71. E. Maris, R. Oostenveld, Nonparametric statistical testing of EEG- and MEG-data. *J. Neurosci. Methods* **164**, 177–190 (2007).

Supplementary Information for

Heart-Brain Interactions Shape Somatosensory Perception and Evoked Potentials

Esra Al, Fivos Iliopoulos, Norman Forschack, Till Nierhaus, Martin Grund,
Paweł Motyka, Michael Gaebler, Vadim V. Nikulin, Arno Villringer

Corresponding authors: Esra Al and Arno Villringer
Emails: esraal@cbs.mpg.de and villringer@cbs.mpg.de

This PDF file includes:

> Supplementary text
> Figures S1 to S8
> Tables S1 to S5
> SI References

1

Supplementary Information Text

Methods

Source reconstruction. Source localization was performed with the BrainStorm toolbox (1) using individually measured electrode positions. When available, individual brain anatomies (19 subjects) and otherwise a template brain anatomy (ICBM152; 2) were used. Cortical surfaces were segmented from structural MRI data (MPRAGE) using Freesurfer (3) and a 3-shell boundary element model (BEM) was constructed to calculate the lead field matrix with OpenMEEG (4). We used eLORETA to compute orientation-constrained sources for each condition and subject (5). The MATLAB code for eLORETA algorithm is available in the MEG/EEG Toolbox of Hamburg (METH; https://www.uke.de/english/departments-institutes/institutes/neurophysiology-and-pathophysiology/research/research-groups/index.html). Individual source data were then projected to the ICBM152 template (2). Cortical anatomy was segmented according to Destrieux atlas (6).

General linear mixed-effects modeling (GLMM). This method was used for mediation analyses since they both acknowledge both between- and within-participant variations in the data from the model's fixed-effect estimates. GLMM was conducted in R (R Core Team, 2014) within the lme4 framework (7). The models were defined in the following form: outcome ~ predictor(s) + (predictor(s) | subject), which fits predictors of the fixed effect part (next to the "~") and predictors of the random effects part (in brackets) grouped by a factor, for which the predictors vary randomly, in our case, subjects.

First, we used GLMM to test whether the cardiac phase effect on detection was mediated by the prestimulus alpha amplitude. We computed five GLMMs regressing detection outcome (hit or miss): (1) one null model assuming no relationship, i.e., only the intercept served as predictor; (2,3) two models including either cardiac phase or alpha amplitudes as the fixed and random effect to regress detection; (4) an additive model regressing detection on both cardiac phase and alpha amplitude and (5) an interactive model assuming an interaction between cardiac phase and alpha amplitude to regress detection (see **Table S4**). Second, we used GLMM to test whether prestimulus alpha mediated the effect of HEP on detection. We computed five GLMMs regressing detection outcome: (6) one null model; (7,8) two models including either HEP or alpha amplitudes as the fixed and random effect to regress detection; (9) an additive model regressing detection on both HEP and (10) alpha amplitude and an interactive model assuming an interaction between these two predictors (see **Table S5**). In all the models containing alpha as a predictor, we used natural logarithmic transformation of alpha amplitude to normalize its distribution. To determine the best GLMM model explaining the data, maximum-likelihood ratio test statistics, which account for model complexity, were used.

Supplementary GLMM Results
To test the relationship between prestimulus sensorimotor alpha amplitude, cardiac phase and detection, general linear mixed-effects modeling (GLMM) regressions were fitted at the single-trial level. Regressions that included only the cardiac phase or only the alpha amplitude were highly significant compared to a null model, i.e., a model with no relationship assumed (*cardiac model*: $\chi^2 = 18.07$, $p = 4 \cdot 10^{-4}$; *alpha$_1$ model*: $\chi^2 = 121.71$, $p = 2 \cdot 10^{-16}$; **Table S4**). The comparison of the *alpha$_1$ model* and the *cardiac model* favored the *alpha$_1$ model* ($\chi^2 = 103.64$, $p = 2 \cdot 10^{-16}$; **Table S4**). The *additive$_1$ model* that included both cardiac phase and alpha amplitude fitted the data significantly better than the *alpha$_1$ model* ($\chi^2 = 17.41$, $p = 0.002$) and an *interaction$_1$ model* that included an interaction between cardiac phase and alpha ($\chi^2 = 1.51$, $p = 0.91$; **Table S4**). To illustrate the best model, the *additive$_1$ model,* with numbers: If a stimulus was preceded by an alpha amplitude of 0.5 µV (1 standard deviation below the mean amplitude), the detection rates for stimuli in diastole and systole would be 56% and 53%, respectively. When prestimulus alpha amplitude increased to 1.4 µV (1 standard deviation above the mean amplitude), the detection rates for stimuli in diastole and systole would decrease to 49% and 46%, respectively. In summary, these results suggest that sensorimotor alpha and cardiac phase have independent effects on detection, i.e., alpha is not mediating the effect of cardiac phase on somatosensory detection.

Similarly, to confirm the additive effect of the amplitudes of prestimulus sensorimotor alpha and HEP on detection at the single-trial level, we calculated GLMM regression fits (cf. previous section). Regressions that included only alpha or only HEP, respectively, as predictors were highly significant compared with a null model (*alpha$_2$ model*: (χ^2 = 60.27, *p* = 5·10^{-13}; HEP model: χ^2 = 85.29, *p* = 2·10^{-16}; **Table S5**). The comparison of the *alpha$_2$ model* and the *HEP model* favored the *HEP model* (χ^2 = 25.02, *p* = 2·10^{-16}; **Table S5**). The *additive$_2$ model* including both HEP and alpha amplitude in the regression fitted the data better than the *alpha$_2$ model* (χ^2 = 62.73, *p* = 1·10^{-12}) and the *interaction$_2$ model* (χ^2 = 0.57, *p* = 0.45; **Table S5**). To illustrate the best model, the *additive$_2$ model,* with numbers: If a stimulus was preceded by a HEP amplitude of -1.7µV and an alpha amplitude of 0.5µV (1 standard deviation below the mean amplitude), the probability of detecting a stimulus was 59%. This probability would decrease to 51% if only the HEP amplitude would increase to 1.6µV and to 51% if only the alpha amplitude would increase to 1.4µV. If both HEP and alpha amplitudes would increase to 1.6µV and 1.4µV (one standard deviation above the mean amplitude), respectively, the detection probability would decrease to 43%. The GLMM results further support that sensorimotor alpha and HEP have independent effects on detection. Thus, alpha is also not mediating the effect of HEP on somatosensory detection.
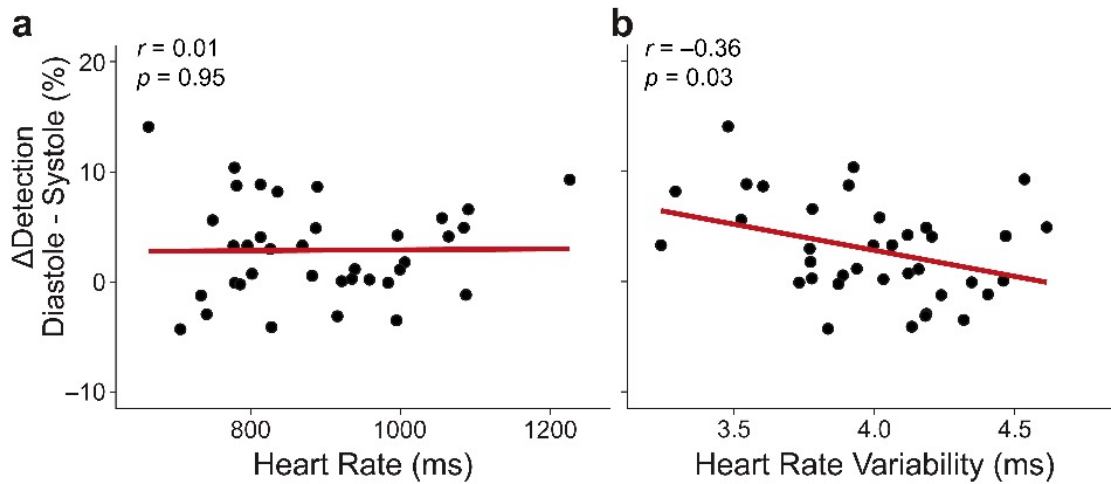
Figure S1. The change of detection between diastole and systole and its correlation with heart rate and heart rate variability. (a) Heart rate of subjects did not significantly correlate with their detection performance change between diastole and systole (Pearson's correlation $r = 0.01$, $p = 0.95$) (b) Heart rate variability (i.e., the standard deviation of RR intervals, SDNN) of subjects negatively correlated with the change of detection performance between systole and diastole ($r = -0.36$, $p = 0.03$).
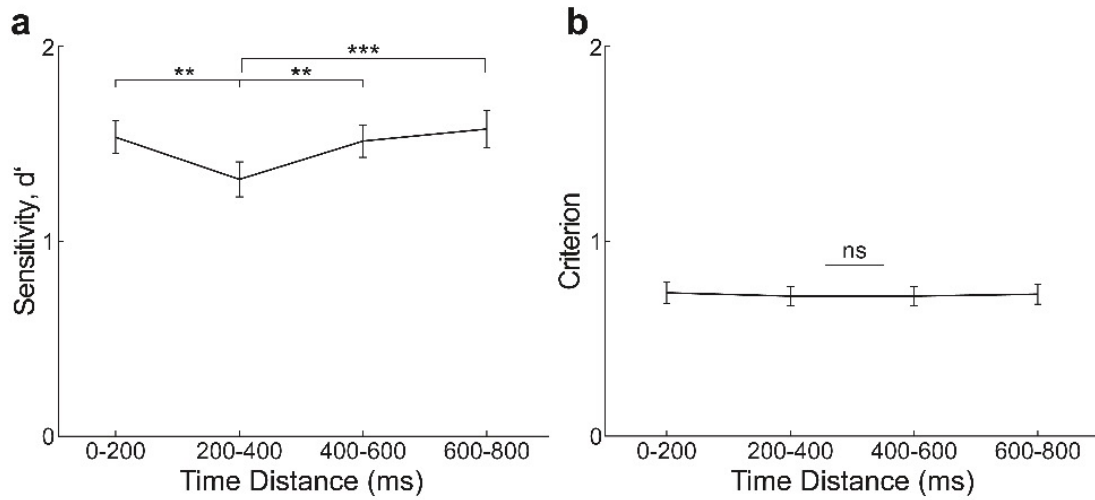
Figure S2. Sensitivity and criterion across four time windows of stimulus onset relative to the previous heartbeat (R-peak). (a) The detection sensitivity (d') was lowest $200-400$ ms after the R-peak (*post-hoc* paired *t*-test between $0-200$ and $200-400$ ms, $t_{36} = 2.83$, $p = 0.008$ and between $200-400$ and $400-600$ ms, $t_{36} = -3.48$, $p = 0.001$) (b) Criterion did not differ significantly between the four time windows (main effect of time, $F_{3,108} = 0.10$, $p = 0.96$). Error bars represent SEMs. **$p < 0.005$, ***$p < 0.0005$. ns, not significant.
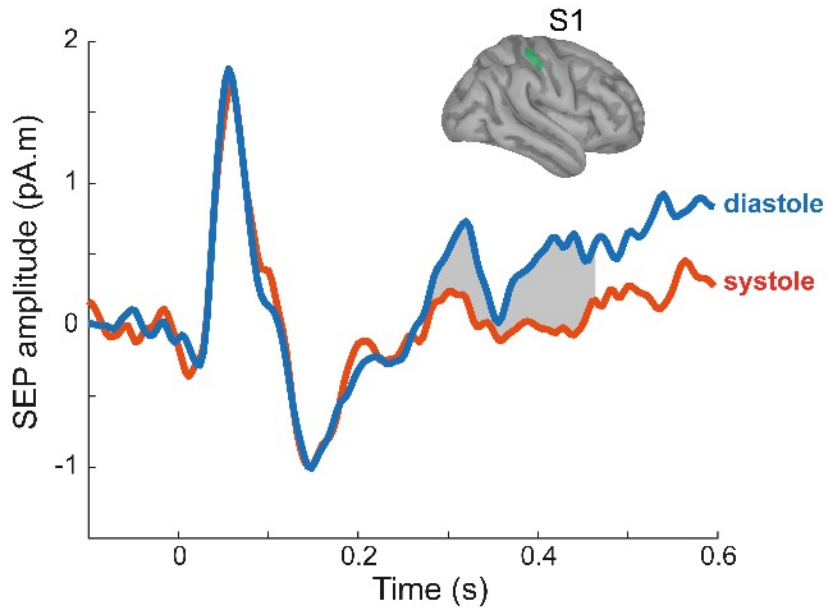
Figure S3. Somatosensory-evoked potentials (SEPs) for stimulations during systole versus diastole in source level. The source-reconstructed P300 amplitude was significantly different between systole and diastole in contralateral somatosensory cortex (S1) similar to the sensory data (t_{36} = -2.55, p = 0.01).
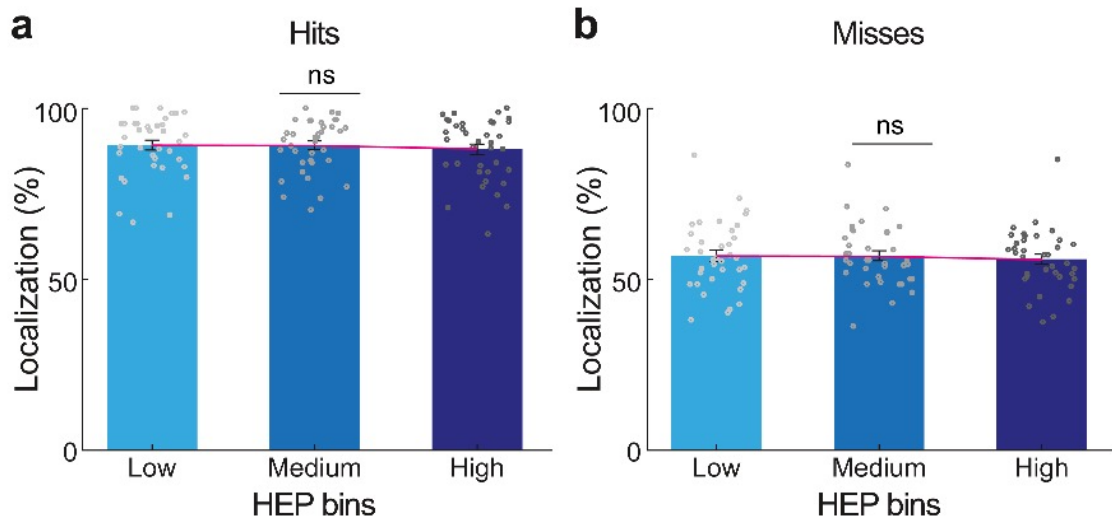
Figure S4. Correct localization of hits and misses across heartbeat-evoked potential (HEP) bins. (**a**) Correct localization of hits did not significantly change across increasing levels of HEP (within-subject ANOVA, $F_{2,72} = 1.26$, $p = 0.29$) (**b**). Correct localization of misses did not significantly vary across HEP bins ($F_{2,72} = 0.28$, $p = 0.76$). Error bars represent SEMs. ns, not significant.
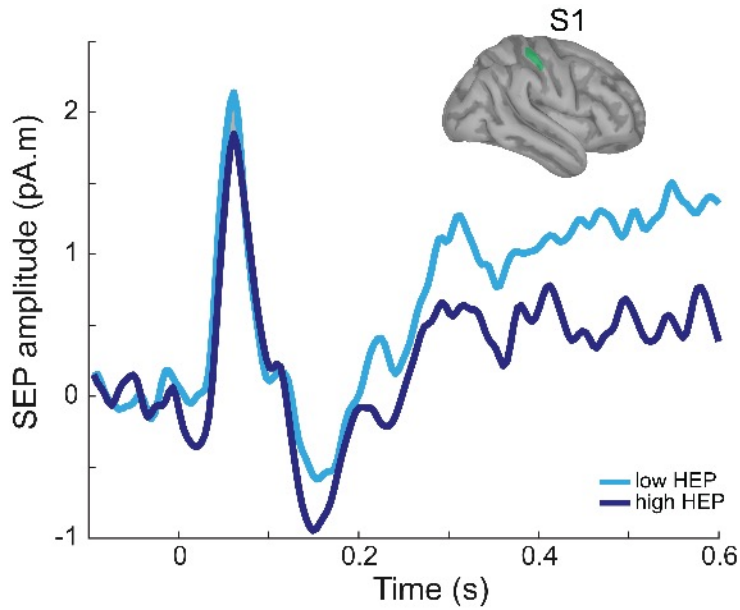
Figure S5. Somatosensory-evoked potentials (SEPs) following low and high HEP amplitudes in source level. A significant difference in P50 amplitude after the low and high HEP amplitudes was observed in the contralateral somatosensory cortex (S1; $t_{36} = 2.15$, $p = 0.03$).
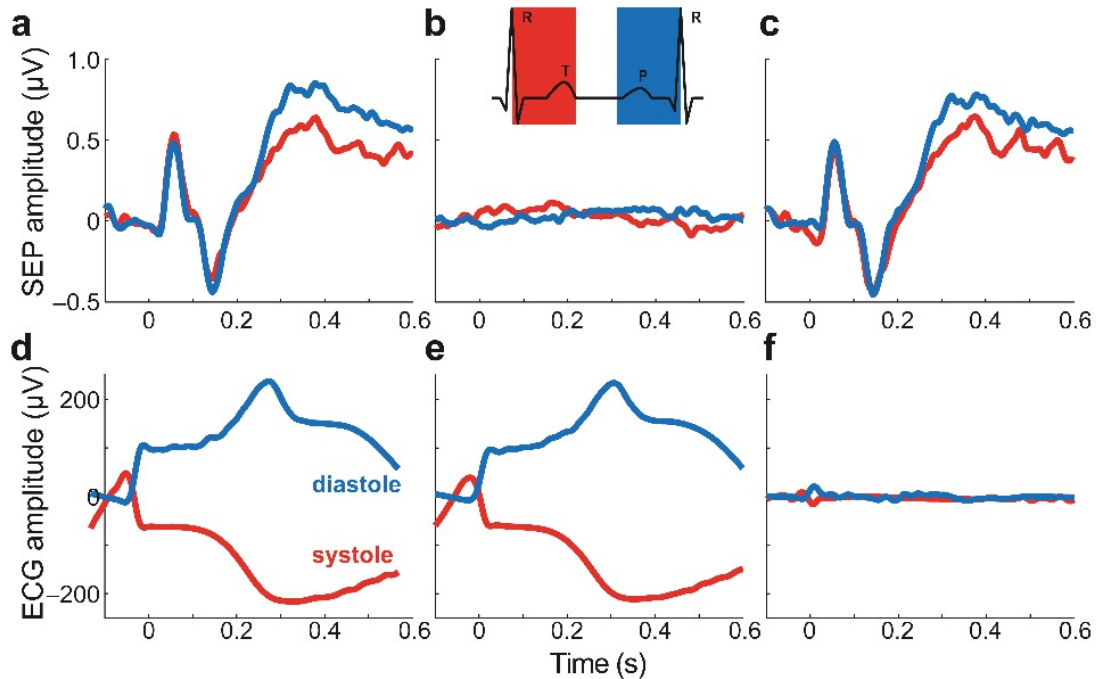
Figure S6. Effect of ECG artifact correction on stimulus-onset locked somatosensory-evoked potential (SEP) and electrocardiogram (ECG) amplitude (0=stimulation onset). (**a**) SEP at C4 before the artifact removal. (**b**) To cancel out the possible effects of ECG artifact, we estimated the cardiac artifact in the evoked responses by first placing random triggers along those cardiac cycles outside the stimulation window of the experiment). Then, we classified the arbitrary triggers as systole or diastole depending on the position of the trigger in the cardiac cycle. After the classification, we segmented data around the triggers and calculated the average cardiac artifact separately for systole and diastole in C4 electrode. (**c**) SEP during systole and diastole after the estimated artifact removal. The average estimation of the cardiac artifact for systole and diastole were subtracted from the SEP separately during systole and diastole. A comparison between uncorrected (a) and corrected SEPs (c) for the ECG artifact indicates that the differences between systole and diastole found between $268-468\,\mathrm{ms}$ is observable regardless of the effect of the correction. (**d**) Stimulus onset-locked ECG, grand average across participants before the artifact removal. (**e**) The estimated average cardiac artifacts on ECG amplitude relative to random triggers placed along the cardiac cycles excluding the stimulation window. (**f**) After the subtraction of the estimated cardiac artifact from the stimulus onset-locked ECG activity separately for systole and diastole, the difference in ECG amplitude during diastole versus systole is negligible. This analysis shows that the observed SEP differences between diastole and systole after ECG correction cannot be attributed to differences in cardiac electrical activity.
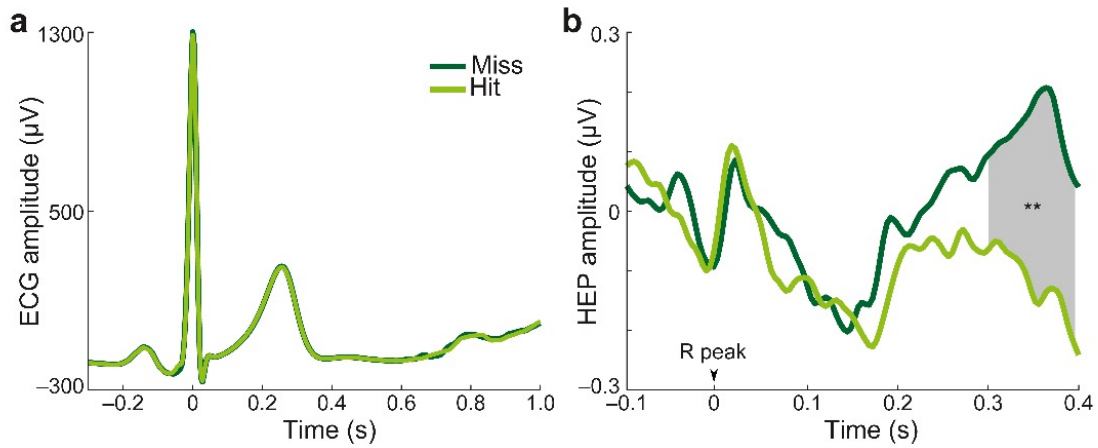
9

Figure S7. The difference of heartbeat-evoked potential (HEP) amplitude between hits and misses is not due to a cardiac field artifact (**a**) R-peak locked electrocardiogram (ECG) grand average across participants. We did not find any significant difference in ECG data between hits and misses (**b**) The HEP across cluster electrodes before cardiac field artifact removal with independent component analysis. The significant difference of HEP between hits and misses between 296–400 ms (gray area) after the R-peak was conserved. This shows that the artifact correction did not induce changes in the reported HEP-related effects. Furthermore, it suggests that the observed HEP-related effects are not likely to occur due to a volume conduction problem. **$p < 0.005$.

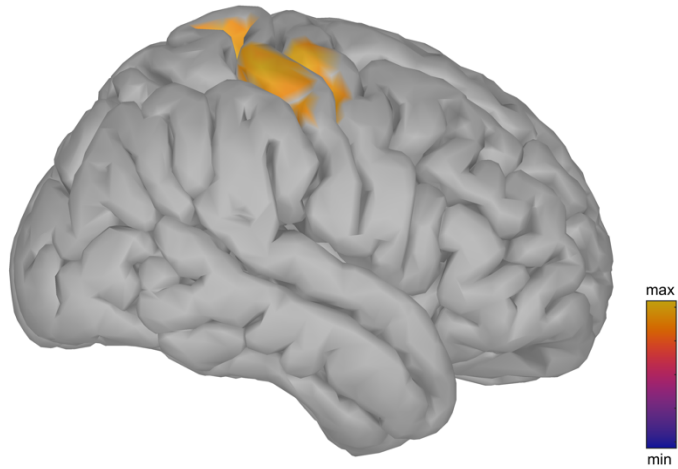**Figure S8.** Source localization of sensorimotor ICA components. Sources were reconstructed for ICA components representing sensorimotor rhythms in every subject. Then, the grand average of source activity across subjects was calculated. The figure shows that source activity originates from the contralateral sensorimotor cortex with a maximum in the somatosensory hand area. The visualized activity represents >75% of source strengths.

Table S1. The electrical stimulus intensities (in mA) applied to the index and the middle finger during systole and diastole

	Systole	Diastole	t_{36}	p
Index	2.04 ± 0.64	2.04 ± 0.64	0.35	0.73
Middle	2.26 ± 0.74	2.26 ± 0.75	0.25	0.80
Overall	2.15 ± 0.67	2.15 ± 0.69	0.57	0.57

Table S2 Comparison of mean P300 amplitude between systole and diastole in source level

	t_{36}	p
Anterior Insula (R)	-0.71	0.48
Anterior Cingulate Cortex (R)	1.31	0.20
Anterior Cingulate Cortex (L)	-0.31	0.76
Posterior Cingulate Cortex (R)	2.15	0.04
Posterior Cingulate Cortex (L)	-0.37	0.72
Inferior Parietal Lobule (R)	1.02	0.32
Lateral Prefrontal Cortex (R)	1.06	0.30
Lateral Prefrontal Cortex (L)	1.14	0.26

None of these regions demonstrated significant differences after FDR correction.

Table S3 Comparison of mean P50 amplitudes following low and high HEP amplitudes in source level

	t_{36}	p
Anterior Insula (R)	**3.83**	**5·10⁻⁴**
Anterior Cingulate Cortex (R)	-0.17	0.87
Anterior Cingulate Cortex (L)	0.37	0.71
Posterior Cingulate Cortex (R)	**-3.39**	**2·10⁻³**
Posterior Cingulate Cortex (L)	**-4.55**	**6·10⁻⁵**
Inferior Parietal Lobule (R)	1.36	0.18
Lateral Prefrontal Cortex (R)	**-4.14**	**2·10⁻⁴**
Lateral Prefrontal Cortex (L)	**-3.80**	**5·10⁻⁴**

The highlighted regions demonstrated significant differences after FDR correction.

Table S4 General linear mixed-effects modeling (GLMM) testing the relationship between prestimulus alpha amplitude, cardiac phase, and detection (model no. 1-5)

Model name	Glmer syntax	Likelihood	LRT
1 – $null_1$	detection ~ 1 + (1 | subject)	-14,165	
2 – cardiac	detection ~ cardiac + (cardiac | subject)	-14,156	(1) $\chi2 = 18.07$***
3 – $alpha_1$	detection ~ alpha + (alpha | subject)	-14,104	(1) $\chi2 = 121.71$***
			(2) $\chi2 = 103.64$***
4 – $additive_1$	detection ~ cardiac + alpha + (cardiac + alpha | subject)	-14,096	(3) $\chi2 = 17.41$**
5 – $interaction_1$	detection ~ cardiac * alpha + (cardiac * alpha | subject)	-14,095	(4) $\chi2 = 1.51$

Likelihood shows the log-transformed likelihood of the models. Higher values of likelihood make the model more likely. LRT is the maximum likelihood ratio test comparing two models for the same dataset. More complex models (with more parameters) are compared with respective smaller ones, which gives a *χ2* and *p*-value. *$p < 0.05$, **$p < 0.005$, *** $p < 0.0005$.

Table S5 General linear mixed-effects modeling (GLMM) testing the relationship between prestimulus sensorimotor alpha amplitude, heartbeat-evoked potential, and detection (model no. 6-10)

Model name	Glmer syntax	Likelihood	LRT
6 – null$_2$	detection ~ 1 + (1 | subject)	- 10,007	
7 – alpha$_2$	detection ~ alpha + (alpha | subject)	- 9,976	(6) $\chi2 = 60.27$***
8 – HEP	detection ~ HEP + (HEP | subject)	- 9,964	(6) $\chi2 = 85.29$***
			(7) $\chi2 = 25.02$***
9 – additive$_2$	detection ~ HEP + alpha + (HEP + alpha | subject)	- 9,933	(8) $\chi2 = 62.73$***
10 – interaction$_2$	detection ~ HEP * alpha + (HEP * alpha | subject)	- 9,932	(9) $\chi2 = 0.57$

Models are evaluated as in Table 2. *$p < 0.05$, **$p < 0.005$, *** $p < 0.0005$.

References

1. F. Tadel, S. Baillet, J. C. Mosher, D. Pantazis, R. M. Leahy, Brainstorm: A user-friendly application for MEG/EEG analysis. *Comput. Intell. Neurosci.* **2011** (2011).
2. V. Fonov, A. Evans, R. McKinstry, C. Almli, D. Collins, Unbiased nonlinear average age-appropriate brain templates from birth to adulthood. *Neuroimage* **47**, S102 (2009).
3. B. Fischl, FreeSurfer. *Neuroimage* **62**, 774–781 (2012).
4. A. Gramfort, T. Papadopoulo, E. Olivi, M. Clerc, OpenMEEG: opensource software for quasistatic bioelectromagnetics. *Biomed. Eng. Online* **9**, 45 (2010).
5. R. D. Pascual-Marqui, Discrete, 3D distributed, linear imaging methods of electric neuronal activity. Part 1: exact, zero error localization (2007) (January 17, 2020).
6. C. Destrieux, B. Fischl, A. Dale, E. Halgren, Automatic parcellation of human cortical gyri and sulci using standard anatomical nomenclature. *Neuroimage* **53**, 1–15 (2010).
7. D. Bates, M. Mächler, B. Bolker, S. Walker, Fitting Linear Mixed-Effects Models Using lme4. *J. Stat. Software; Vol 1, Issue 1* (2015) https:/doi.org/10.18637/jss.v067.i01.

6 Curriculum Vitae

My curriculum vitae does not appear in the electronic version of my paper for reasons of data protection.

7 Complete List of Publications

7.1 Peer-Reviewed Original Research Articles

<u>Publication 1:</u> **Al, E.**, Iliopoulos, F., Forschack, N., Nierhaus, T., Grund, M., Motyka, P., Gaebler, M., Nikulin, V. V. & Villringer, A. Heart-brain interactions shape somatosensory perception and evoked potentials. *Proc. Natl. Acad. Sci. U. S. A.* **117,** 10575–10584 (2020). Impact Factor (2018) = 9.580

<u>Publication 2:</u> Motyka, P., Grund, M., Forschack, N., **Al, E.**, Villringer, A. & Gaebler, M. Interactions between cardiac activity and conscious somatosensory perception. *Psychophysiology* e13424 (2019). Impact Factor (2018) = 3.378

<u>Publication 3:</u> Kumral, D., Şansal, F., Cesnaite, E., Mahjoory, K., **Al, E.**, Gaebler, M., Nikulin, V. V. & Villringer, A. BOLD and EEG signal variability at rest differently relate to aging in the human brain. *Neuroimage* **207,** (2020). Impact Factor (2018) = 5.812

7.2 Preprints

<u>Preprint:</u> **Al, E.**, Iliopoulos, F., Nikulin, V. V & Villringer, A. Heartbeat and Somatosensory Perception. *bioRxiv* 2020.12.29.424693 (2020). doi:10.1101/2020.12.29.424693 (under review)

7.3 Selected Oral and Poster Presentations

Oral Presentations

- **Al E.**, Iliopoulos F., Stephani T., Forster C., Nikulin V V., Villringer A., Somatosensory Localization in the Absence of Conscious Detection, *Neuromatch Conference,* (2020). Online
- **Al, E.**, Iliopoulos, F., Forschack, N., Nierhaus, T., Grund, M., Motyka, P., Gaebler, M., Nikulin, V. V. & Villringer, A., Heart–Brain Interactions Shape Somatosensory Perception and Evoked Potentials. *Interoception Meeting*, (2020). University College of London, Online

- **Al, E.**, Iliopoulos, F., Forschack, N., Nierhaus, T., Grund, M., Motyka, P., Gaebler, M., Nikulin, V. V. & Villringer, A., How Does the Heartbeat Affect Somatosensory Perception?. *Neuroxillations Journal Club*, (2020). University of Oxford, Online
- **Al, E.**, Iliopoulos, F., Forschack, N., Nierhaus, T., Grund, M., Motyka, P., Gaebler, M., Nikulin, V. V. & Villringer, A., Somatosensory Perception Varies Across the Cardiac Cycle. Association for the Scientific Study of Consciousness, (2018). Krakow

Poster Presentations

- **Al E.**, Iliopoulos F., Stephani T., Forster C., Nikulin V V., Villringer A., Neural Correlates of Numbtouch in Healthy Subjects, *The Organization for Human Brain Mapping*, (2020), Online.
- **Al, E.**, Iliopoulos, F., Forschack, N., Nierhaus, T., Grund, M., Motyka, P., Gaebler, M., Nikulin, V. V. & Villringer, A., Somatosensory Perception Varies Across the Cardiac Cycle. *MindBrainBody Symposium*, (2019), Berlin.
- **Al, E.**, Iliopoulos, F., Forschack, N., Nierhaus, T., Grund, M., Motyka, P., Gaebler, M., Nikulin, V. V. & Villringer, A., Somatosensory Detection and Localization Across the Cardiac Cycle. *CuttingEEG conference*, (2018), Paris.
- **Al, E.**, Iliopoulos, F., Forschack, N., Nierhaus, T., Grund, M., Motyka, P., Gaebler, M., Nikulin, V. V. & Villringer, A., Somatosensory Detection and Localization Across the Cardiac Cycle. *Society for Neuroscience,* (2018), San Diego.
- **Al, E.**, Iliopoulos, F., Forschack, N., Nierhaus, T., Grund, M., Motyka, P., Gaebler, M., Nikulin, V. V. & Villringer, A., Do Somatosensory Detection and Localization Vary Across the Cardiac Cycle?. *MindBrainBody Symposium*, (2017), Berlin.

8 Acknowledgments

Throughout my doctoral studies, I was very lucky to be encircled with wonderful people, without whom this thesis would not be possible. First of all, the role of my supervisor, Prof. Dr. Arno Villringer, in my doctoral life was tremendous. I cannot thank him enough for not only guiding me and sharing his knowledge but also being caring and kind. I will always stay thankful to him for giving me the chance to realize my dreams and teaching me a rigorous approach to science. I am also grateful to Dr. Vadim Nikulin, who has been always supportive and encouraging in my path. Every discussion I had with him was inspiring and invaluable for my thesis. Further, I would like to thank to Dr. Michael Gaebler and Prof. Dr. Felix Blankenburg for their support and guidance.

I would like to also thank my colleagues and friends from the somatosensory group at the Max Planck Institute for Human Cognitive and Brain Sciences: Tilman Stephani, Martin Grund, Till Nierhaus, Norman Forschack, Fivos Iliopoulos, Carina Forster, Eleni Panagoulos, Anahit Babayan for providing endless support throughout the years. I also would like to thank to Luke Tudge for his warm support throughout my PhD.

Also, I would like to express my gratitude towards my dear friends for giving me strength and encouragement. Among them, I would like to mention especially: Melina Engelhardt, Işıl Uluç, Enise İncesoy, Stella Kunzendorf, Sedef Karayel, Juan R. Loiza, Caitlin Duncan and Şeyma Bayrak. Furthermore, I would like to specially share my gratitude to Dan J. Cook, who not only inspired me with his challenging scientific questions, but also helped me stand up during difficult times. His emotional support was indispensable for me.

Last but not least, I am grateful to my family for their endless support throughout my life. I would like to say few words to them to express my gratitude in Turkish. Canım babam, bana dünyada doğruları arama ve bilginin peşinde koşma azmini verdiğin için, anneciğim, eğitimimi her şeyin üzerinde tuttuğun ve kendi ayaklarım üzerinde durmama destek olduğun için ve ablacığım, beni bilim insanı olma yolunda cesaretlendirdiğin için çok teşekkür ederim. İyi ki varsınız!